Weak precipitation, warm winters and springs impact glaciers of south slopes of Mt. Everest (central Himalaya) in the last two decades (1994-2013)

Franco Salerno[(1,4*)], Nicolas Guyennon[(2)], Sudeep Thakuri[(1,4)], Gaetano Viviano[(1)], Emanuele Romano[(2)], Elisa Vuillermoz[(4)], Paolo Cristofanelli[(3,4)], Paolo Stocchi[(3)], Giacomo Agrillo[(3)], Yaoming Ma[(5)], Gianni Tartari[(1,4)]

[(1)] National Research Council, Water Research Institute, Brugherio (IRSA -CNR), Italy
[(2)] National Research Council, Water Research Institute, Roma (IRSA-CNR), Italy
[(3)] National Research Council, Institute of Atmospheric Sciences and Climate (ISAC-CNR) Bologna, Italy
[(4)] Ev-K2-CNR Committee, Via San Bernardino, 145, Bergamo 24126, Italy
[(5)] Institute of Tibetan Plateau Research, Chinese Academy of Science, China

Correspondence to Franco Salerno

Email: salerno@irsa.cnr.it
Address: IRSA-CNR Via Del Mulino 19. Località Occhiate 20861Brugherio (MB)
Phone: +39 039 21694221
Fax: +39 039 2004692

Abstract

Studies on recent climate trends from the Himalayan range are limited, and even completely absent at high elevation. This contribution specifically explores the southern slopes of Mt. Everest (central Himalaya), analyzing the minimum, maximum, and mean temperature and precipitation time series reconstructed from seven stations located between 2660 and 5600 m a.s.l. over the last twenty years (1994-2013). We complete this analysis with data from all the existing ground weather stations located on both sides of the mountain range (Koshi Basin) over the same period. Overall we observe that the main and more significant increase in temperature is concentrated outside of the monsoon period. At higher elevations minimum temperature (0.072 ± 0.011 °C a, $p < 0.001$) increased far more than maximum temperature (0.009 ± 0.012 °C a^{-1}, $p > 0.1$), while mean temperature increased by 0.044 ± 0.008 °C a^{-1}, $p < 0.05$. Moreover, we note a substantial precipitation weakening (9.3 ± 1.8 mm a^{-1}, $p < 0.01$ during the monsoon season). The annual rate of decrease at higher elevation is similar to the one at lower altitudes on the southern side of the Koshi Basin, but here the drier conditions of this remote environment make the fractional loss much more consistent (47% during the monsoon period). This study contributes to change the perspective on how the climatic driver (temperature vs. precipitation) led the glacier responses in the last twenty years. The main implications are the following: 1) the negative mass balances of glaciers observed in this region can be more ascribed to less accumulation due to weaker

precipitation than to an increase of melting processes. 2) The melting processes have only been favored during winter and spring months and close to the glaciers terminus. 3) A decreasing of the probability of snowfall has significantly interested only the glaciers ablation zones (10 %, $p < 0.05$), but the magnitude of this phenomenon is decidedly lower than the observed decrease of precipitation. 4) The lesser accumulation could be the cause behind the observed lower glacier flow velocity and the current stagnation condition of tongues, which in turn could have trigged melting processes under the debris glacier coverage, leading to the formation of numerous supraglacial and proglacial lakes that have characterized the region in the last decades. Without demonstrating the causes that could have led to the climate change pattern observed at high elevation, we conclude by listing the recent literature on hypotheses that accord with our observations.

Keywords: temperature lapse rate, precipitation gradient, monsoon weakening, Sequential Mann-Kendall, expectation maximization algorithm, climate change, glaciers shrinkage, central Himalaya

1 Introduction

The current uncertainties concerning the glacial shrinkage in the Himalayas are mainly attributed to a lack of measurements, both of the glaciers and of climatic forcing agents (e.g., Bolch et al., 2012). Recent results underline the need for a fine scale investigation, especially at high altitude, to better model the hydrological dynamics in this area. However, there are few high elevation weather stations in the world where the glaciers are located (Tartari et al., 2009). This can be attributed to the remote location of glaciers, the rugged terrain, and a complex political situation, all of which make physical access difficult (Bolch et al., 2012). As a consequence of the remoteness and difficulty in accessing many high elevation sites combined with the complications of operating automated weather stations (AWSs) at these altitudes, long-term measurements are challenging (Vuille, 2011). However, nearly all global climate models report increased sensitivity to warming at high elevations (e.g., Rangwala and Miller, 2012), while observations are less clear (Pepin and Lundqist, 2008). Moreover, changes in the timing or amount of precipitation are much more ambiguous and difficult to detect, and there is no clear evidence of significant changes in total precipitation patterns in most mountain regions (Vuille, 2011).

The need for a fine scale investigation is particularly evident on the south slope of Mt. Everest (central Southern Himalaya, CH-S) as it is one of the heavily glaciated parts of the Himalaya (Salerno et al., 2012; Thakuri et al., 2014). Nevertheless, these glaciers have the potential to build up moraine-dammed lakes storing large quantities of water, which are susceptible to GLOFs (glacial lake outburst floods) (e.g., Salerno et al., 2012; Fujita et al., 2013). Gardelle et al. (2011) noted that this region is most characterized by glacial lakes in the Hindu Kush Karakorum Himalaya. Recently, Thakuri et al. (2014) noted that the Mt. Everest glaciers experienced an accelerated shrinkage in the last

twenty years (1992-2011), as underlined by an upward shift of the Snow Line Altitude (SLA) with a velocity almost three times greater than the previous period (1962-1992). Furthermore Bolch et al. (2011) and Nuimura et al. (2012) found a higher mass loss rate during the last decade (2000–2010). Anyway, to date, there are not continuous meteorological time series able to clarify the causes of the melting process to which the glaciers of these slopes are subjected.

In this context, since the early 1990s, PYRAMID Observatory Laboratory (5050 m) was created by the EV-K2-CNR Committee (www.evk2cnr.org). This observatory is located at the highest elevation at which weather data has ever been collected in the region and thus represents a valuable dataset with which to investigate the climate change in CH-S (Tartari et al., 2002; Lami et al., 2010). However, the remoteness and the harsh conditions of the region over the years have complicated the operations of the AWSs, obstructing long-term measurements from a unique station.

In this paper, we mainly explore the small scale climate variability of the south slopes of Mt. Everest by analyzing the minimum, maximum, and mean air temperature (T) and precipitation (Prec) time series reconstructed from seven AWSs located from 2660 to 5600 m a.s.l. over the last couple of decades (1994-2013). Moreover, we complete this analysis with all existing weather stations located on both sides of the Himalayan range (Koshi Basin) for the same period. In general, this study has the ultimate goal of linking the climate change patterns observed at high elevation with the glacier responses over the last twenty years, during which a more rapid glacier shrinkage process occurred in the region of investigation.

2 Region of investigation

The current study is focused on the Koshi (KO) Basin which is located in the eastern part of central Himalaya (CH) (Yao et al., 2012; Thakuri et al., 2014). To explore possible differences in the surroundings of Mt. Everest, we decided to consider the north and south parts of CH (with the suffixes -N and –S, respectively) separately (Fig. 1a). The KO River (58,100 km^2 of the basin) originates in the Tibetan Plateau (TP) and the Nepali highlands. The area considered in this study is within the latitudes of 27° and 28.5° N and longitudes of 85.5° and 88° E. The altitudinal gradient of this basin is the highest in the world, ranging from 77 to 8848 m a.s.l., i.e., Mt. Everest. We subdivide the KO Basin into the northern side (KO-N), belonging to the CH-N, and southern side (KO-S), belonging to the CH-S. The southern slopes of Mt. Everest are part of the Sagarmatha (Everest) National Park (SNP) (Fig. 1b), where the small scale climate variability at high elevation is investigated. The SNP is the world's highest protected area, with over 30000 tourists in 2008 (Salerno et al., 2013). The park area (1148 km^2), extending from an elevation of 2845 to 8848 m a.s.l., covers the upper Dudh Koshi (DK) Basin (Manfredi et al., 2010; Amatya et al., 2010). Land cover classification shows that almost one-third of the territory is characterized by glaciers and ice cover (Salerno et al., 2008; Tartari et al., 2008), while less than 10% of the park area is forested (Bajracharya et al., 2010). The SNP presents a broad range of bioclimatic

conditions with three main bioclimatic zones: the zone of alpine scrub; the upper alpine zone, which includes the upper limit of vegetation growth; and the Arctic zone, where no plants can grow (UNEP and WCMC, 2008). Figure 1c shows the glacier distribution along the hypsometric curve of the SNP. We observe that the glacier surfaces are distributed from 4300 m to above 8000 m a.s.l., with more than 75% of the glacier surfaces lying between 5000 m and 6500 m a.s.l. The 2011 area-weighted mean elevation of the glaciers was 5720 m a.s.l. (Thakuri et al., 2014). These glaciers are identified as the summer accumulation-type fed mainly by summer Prec from the South Asian monsoon system, whereas the winter Prec caused by the mid-latitude westerly wind is minimal (Yao et al., 2012). The prevailing direction of the monsoons is S-N and SW-NE (e.g., Ichiyanagi et al., 2007). The climate is influenced by the monsoon system because the area is located in the subtropical zone with nearly 90% of the annual Prec falling in the months of June to September (this study). Heavy autumn and winter snowfalls can occur in association with tropical cyclones and westerly disturbances, respectively, and snow accumulation can occur at high elevations at all times of the year (Benn, 2012). Bollasina et al. (2002) have demonstrated the presence of well-defined local circulatory systems in the Khumbu Valley (SNP). The local circulation is dominated by a system of mountain and valley breezes. The valley breeze blows (approximately 4 m s^{-1}) from the south every day from sunrise to sunset throughout the monsoon season, pushing the clouds that bring Prec northward.

3 Data

3.1 Weather stations at high elevation

The first automatic weather station (named hereafter AWS0) at 5050 m a.s.l. near PYRAMID Observatory Laboratory (Fig. 1c), and beginning in October 1993, it has run continuously all year round (Bertolani et al., 2000). The station, operating in extreme conditions, had recorded long-term ground-based meteorological data, and these data are considered valid until December 2005. Due to the obsolescence of technology, the station was disposed of in 2006. A new station (named hereafter AWS1) was installed just a few tens of meters away from AWS0 and has been operating since October 2000. Other stations were installed in the following years in the upper DK Basin in the Khumbu Valley (Table 1). In 2008, the network included the sixth monitoring point, the highest weather station of the world, located at South Col of Mt. Everest (7986 m a.s.l.). The locations of all stations are presented in Figure 1b. We can observe in Figure 1c that this meteorological network represents the climatic conditions of the SNP glaciers well. AWS0 and AWS1 (5035 m a.s.l.) characterize the glacier fronts (4870 m a.s.l.), AWS4 (5600 m a.s.l.) represents the mean elevation of glaciers (5720 m a.s.l.), and AWS5, the surface station at South Col (7986 m a.s.l.), characterizes the highest peaks (8848 m a.s.l.).

All stations, except AWS5, record at least T and Prec. This dataset presents some gaps (listed in Table 1) as a consequence of the complications of operating AWS at these

altitudes. The list of measured variables for each stations and relevant data can be downloaded from http://geonetwork.evk2cnr.org/. Data processing and quality checks are performed according to the international standards of the WMO (World Meteorological Organization).

The Prec sensors at these locations are tipping buckets usually used for rainfall measurements and may not fully capture the solid Prec. Therefore, Prec is probably underestimated, especially in winter. In this regard, according to both Fujita and Sakai, 2014 and field observations (Ueno et al., 1994), the precipitation phase has been taken into account assuming that the probability of snowfall and rainfall depends on mean daily temperature, using – as proposed by the aforementioned authors – as thresholds 0 °C and 4 °C, respectively. In Figure 2 we first of all observe that at 5050 m a.s.l. 90% of precipitation is concentrated during June-September and that the probability of snowfall is very low (4%), considering that the mean daily temperature during these months is above 0 °C. On a yearly basis, this probability reaches 20% of the annual cumulated precipitation.

3.2 Other weather stations at lower altitude in the Koshi Basin

In KO-S Basin (Nepal), the stations are operated by the Department of Hydrology and Meteorology (DHM) (www.dhm.gov.np/). For daily T and Prec, we selected 10 stations for T and 19 stations for Prec considering both the length of the series and the monitoring continuity (< 10% of missing daily data). The selected stations cover an elevation range between 158 and 2619 m a.s.l. (Table 3). In KO-N Basin (TP, China), the number of ground weather stations (operated by the Chinese Academy of Science (CAS)), selected with the same criteria mentioned above, is considerably smaller, just two, but these stations have a higher elevation (4302 m for the Dingri station and 3811 m a.s.l. for the Nyalam station).

4 Methods

We define the pre-monsoon, monsoon, and post-monsoon seasons as the months from February to May, June to September, and October to January, respectively. The minT, maxT, and meanT are calculated as the minimum, maximum, and mean daily air temperature. For total precipitation (Prec), we calculate the mean of the cumulative precipitation for the analyzed period.

4.1 Reconstruction of the daily temperature and precipitation time series at high elevation

The two stations named AWS0 and AWS1 in the last twenty years, considering the extreme weather conditions of these slopes, present a percentage of missing daily values of approximately 20% (Table 1). The other stations (hereafter named secondary stations) were used here for infilling the gaps according to a priority criteria based on

196 the degree of correlation among data. AWS1 was chosen as the reference station given
197 the length of the time series and that it is currently still operating. Therefore, our
198 reconstruction (hereafter named PYRAMID) is referred to an elevation of 5035 m a.s.l.
199 The selected infilling method is a simple regression analysis based on quantile
200 mapping (e.g., Déqué, 2007; Themeßl et al., 2012). This simple regression method has
201 been preferred to more complex techniques, such as the fuzzy rule-based approach
202 (Abebe et al., 2000) or the artificial neural networks (Abudu et al., 2010; Coulibaly and
203 Evora, 2007), considering the peculiarity of this case study. In fact, all stations are
204 located in the same valley (Khumbu Valley). This aspect confines the variance among
205 the stations to the altitudinal gradient of the considered variable (T or Prec), which can
206 be easily reproduced by the stochastic link created by the quantile mapping method. In
207 case all stations registered a simultaneous gap, we apply a multiple imputation
208 technique (Schneider, 2001) that uses some other proxy variables to fill the remaining
209 missing data. Details on the reconstruction procedure and the computation of the
210 associated uncertainty are provided in Supplementary Material 1.

211 4.2 The trends analysis: the Sequential Mann-Kendall test

212 The Mann-Kendall (MK) test (Kendall, 1975) is widely adopted to assess significant
213 trends in hydro-meteorological time series (e.g., Carraro et al., 2012a, 2012b; Guyennon
214 et al., 2013). This test is non-parametric, thus being less sensitive to extreme sample
215 values, and is independent of the hypothesis about the nature of the trend, whether
216 linear or not. The MK test verifies the assumption of the stationarity of the investigated
217 series by ensuring that the associated normalized Kendall's tau coefficient, $\mu(\tau)$, is
218 included within the confidence interval for a given significance level (for $\alpha = 5\%$, the
219 $\mu(\tau)$ is below –1.96 and above 1.96). In the sequential form (seqMK) (Gerstengarde
220 and Werner, 1999), $\mu(\tau)$ is calculated for each element of the sample. The procedure
221 is applied forward starting from the oldest values (progressive) and backward starting
222 from the most recent values (retrograde). If no trend is present, the patterns of
223 progressive and retrograde $\mu(\tau)$ versus time (i.e., years) present several crossing
224 points, while a unique crossing period allows the approximate location of the starting
225 point of the trend (e.g., Bocchiola and Diolaiuti, 2010).
226 In this study, the seqMK is applied to monthly vectors. Monitoring the seasonal non-
227 stationarity, the monthly progressive $\mu(\tau)$ is reported with a pseudo color code, where
228 the warm colors represent the positive slopes and cold colors the negative ones. Color
229 codes associated with values outside of the range (-1.96 to 1.96) possess darker tones to
230 highlight the trend significance (Salerno et al., 2014). Moreover, to monitor the overall
231 non-stationarity of the time series, both the progressive and the retrograde $\mu(\tau)$ at the
232 annual scale are reported. We used the Sen's slope proposed by Sen (1968) as a robust
233 linear regression allowing the quantification of the potential trends revealed by the
234 seqMK (e.g., Bocchiola and Diolaiuti, 2010). The significance level is established for $p < 0.05$. We define a slight significance for $p < 0.10$. The uncertainty associated with the
235

Sen's slopes (1994-2013) is estimated through a Monte Carlo uncertainty analysis (e.g., James and Oldenburg, 1997), described in detail in Supplementary Material 1.

5 Results

5.1 Trend analysis at high elevation

Figure 3 shows the reconstructed PYRAMID time series for minT, maxT, meanT, and Prec resulting from the overall infilling process explained in Supplementary Material 1. Figure 4 analyzes the monthly trends of T and Prec from 1994 to 2013 for PYRAMID.

Minimum air temperature (minT)

November (0.17 °C a^{-1}, $p < 0.01$) and December (0.21 °C a^{-1}, $p < 0.01$) present the highest increasing trend, i.e., both these two months experienced about even +4 °C over twenty years (Fig. 4a). In general, the post- and pre-monsoon periods experience higher and more significant increases than during the monsoon. In particular, we note the significant and consistent increase of April (0.10 °C a^{-1}, $p < 0.05$). At the annual scale, the bottom graph shows a progressive $\mu(\tau)$ trend parallel to the retrograde $\mu(\tau)$ one for the entire analyzed period, i.e., a continuous tendency of minT to rise, which becomes significant in 2007, when the progressive $\mu(\tau)$ assumes values above +1.96. On the right, the Sen's slope completes the analysis, illustrating that minT is increasing at annual level by 0.072 ± 0.011 °C a^{-1}, $p < 0.001$, i.e., +1.44 ± 0.22 °C over twenty years.

Maximum air temperature (maxT)

The post- and pre-monsoon months show larger increases in maxT, but with lower magnitudes and significance than we observe for minT (Fig. 4b). The highest increases occurs also for this variable in April, November and December. Less expected is the decrease of maxT in May (0.08 °C a^{-1}, $p < 0.05$) and during the monsoon months from June to August (0.05 °C a^{-1}, $p < 0.1$). On the annual scale, the bottom graph shows a continuous crossing of the progressive and retrograde $\mu(\tau)$ trends until 2007, i.e., a general stationary condition. From 2007 until 2010, the trend significantly increased, while 2012 and 2013 register a decrease, bringing the progressive $\mu(\tau)$ near the stationary condition. In fact, on the right, the Sen's slope confirms that maxT is at annual level stationary over the twenty years (+0.009 ± 0.012 °C a^{-1}, $p > 0.1$).

Mean air temperature (meanT)

Figure 4c, as expected, presents intermediate conditions for meanT than for minT and maxT. All months, except May and the monsoon months from June and August, register a positive trend (more or less significant). December presents the highest a more significant increasing trend (0.17 °C a^{-1}, $p < 0.01$), while April shows the highest and a more significant increase ($p < 0.10$) during the pre-monsoon period. On the annual scale,

the bottom graph shows that the progressive $\mu(\tau)$ trend has always increased since 2000 and that it becomes significant beginning in 2008. On the right, the Sen's slope concludes this analysis, showing that meanT has been significantly increasing by 0.044 ± 0.008 °C a^{-1}, $p < 0.05$, i.e., +0.88 ± 0.16 °C over twenty years.

Total precipitation (Prec)

In the last years, all cells are blue, i.e., we observe for all months an overall and strongly significant decreasing trend of Prec (Fig. 4d). In general, the post- and pre-monsoon periods experience more significant decreases, although the monsoon months (June-September) register the main Prec losses (e.g. August registers a Prec loss of even 4.6 mm a^{-1}). On the annual scale, the bottom graph shows a continuous decreasing progressive $\mu(\tau)$ trend since 2000 that becomes significant beginning in 2005. On the right, the Sen's slope notes that the decreasing Prec trend is strongly high and significant at annual level (-7 ± 2.4 mm a^{-1}, $p < 0.001$).

The precipitation reduction is mainly due to a reduction in intensity. However during the early and late monsoon rather show a reduction in duration (see further details in Supplementary Material 2).

5.2 Trend analysis in the Koshi Basin

Table 2 provides the descriptive statistics of the Sen's slopes for minT, maxT, meanT, and Prec for the 1994-2013 period for the Koshi Basin. The stations located on the two sides of the Himalayan range are listed separately. For the southern ones (KO-S), we observe that for minT less than half of the stations experience an increasing trend and just three are significant with $p < 0.1$. In general, the minT on the southern side can be defined as stationary (+0.003 °C a^{-1}). Conversely, the maxT shows a decidedly non-stationary condition. All stations present an increasing trend, and even six of the ten are on the significant rise with at least $p < 0.1$. The mean trend is +0.060 °C a^{-1} ($p < 0.10$). Similarly, the meanT shows a substantial increase. Also in this case, six of the ten stations are on the significant rise with at least $p < 0.1$. The mean trend is +0.029 °C a^{-1} ($p < 0.10$). In regards to Prec, we observe that on the KO-S, 14 of the 19 stations present a downward trend. Among them, eight decrease significantly with at least $p < 0.1$. The mean trend is -11.1 mm a^{-1}, i.e., we observe a decreasing of 15% (222 mm) of precipitation fallen in the basin during the 1994-2013 period (1527 mm on average).

The two stations located on the northern ridge (KO-N) show a singularly slight significant rise for minT (0.034 °C a^{-1}, $p < 0.10$ on average) and for maxT (0.039 °C a^{-1}, $p < 0.10$ on average), recording a consequent mean increase of meanT equal to 0.037 °C a^{-1}, $p < 0.05$. As for Prec, we observe that on the KO-N both stations maintain stationary conditions (-0.1 mm a^{-1}).

Table 3 provides the descriptive statistics of the Sen's slopes on a seasonal base. The stations analyzed here are the same as those considered in Table 2. We begin our description with PYRAMID, already analyzed in detail in Figure 4. We confirm with

this seasonal grouping that the main and significant increases of minT, maxT, and meanT are completely concentrated during the post-monsoon period (e.g., 0.124 °C a^{-1}, $p < 0.01$ for meanT). The pre-monsoon period experienced a slighter and not significant increase (e.g., 0.0[5] $p > 0.1$ for meanT). In general, during the monsoon period, T is much more stationary for all three variables (e.g., 0.0[5] $p > 0.1$ for meanT). Considering the other KO-S stations, the main increasing and significant trends of meanT occurred during the pre-monsoon (0.043 °C a^{-1}) and post-monsoon (0.030 °C a^{-1}) season, while the increase during the monsoon is slighter (0.020 °C a^{-1}). The KO-N stations confirm that the main increasing trend of meanT occurred outside the monsoon period that is stationary (+0.013 °C a^{-1}).

As for Prec, PYRAMID and the other KO-S stations show that the magnitude of the Sen's slopes is higher during the monsoon season (-9.3 mm a^{-1} and -8.6 mm a^{-1}, respectively), when precipitation is more abundant. The relatively low snowfall phase of monsoon Prec at PYRAMID (as specified above) makes the decreasing trend observed during the summer more robust than the annual one as devoid of possible undervaluation of snowfall. The northern stations show slight significant decreasing Prec during the winter (-3.3 mm a^{-1}, $p < 0.05$).

5.3 Lapse rates in the southern Koshi Basin

5.3.1 Air temperature gradient

This study, aiming to create a connection between the climate drivers and cryosphere in the Koshi Basin, which presents the highest altitudinal gradient of the world (77 to 8848 m a.s.l.), offers a unique opportunity to calculate T and Prec lapse rates before analyzing their spatial trends. It is worth noting that the T lapse rate is one of the most important variables for modeling meltwater runoff from a glacierized basin using the T-index method (Hock, 2005; Immerzeel et al., 2014). It is also an important variable for determining the form of Prec and its distribution characteristics (e.g., Hock, 2005). Figure 5a presents the lapse rate of the annual meanT in the KO Basin (Nepal) along the altitudinal range of well over 7000 m (865 to 7986 m a.s.l.). We found an altitudinal gradient of -0.60 °C $(100\ m)^{-1}$ on the annual scale with a linear trend ($r^2 = 0.98$, $p < 0.001$). It is known that up to altitudes of approximately 8-17 km a.s.l. in the lower regions of the atmosphere, T decreases with altitude at a fairly uniform rate (Washington and Parkinson, 2005). Kattel and Yao (2013) recently found a lower annual lapse rate for the overall CH-S, but until 4000 m a.s.l.: -0.52 °C $(100\ m)^{-1}$.

Considering that the lapse rate is mainly affected by the moisture content of the air (Washington and Parkinson, 2005), we also calculated the seasonal gradients (not shown here). We found a dry lapse rate of -0.65 °C $(100\ m)^{-1}$ ($r^2 = 0.99$, $p < 0.001$) during the pre-monsoon season when AWS1 registers a mean relative humidity of 62%. A saturated lapse rate during the monsoon season is -0.57 °C $(100\ m)^{-1}$ ($r^2 = 0.99$, $p < 0.001$) with a mean relative humidity of 96%. During the post-monsoon period, we found a lapse rate equal to that registered during the monsoon: -0.57 $(100\ m)^{-1}$ (r^2 =

0.98, $p < 0.001$) even if the relative humidity is decidedly lower in these months (44%). Kattel and Yao (2013) explain this anomalous low post-monsoon lapse rate as the effect of strong radiative cooling in winter.

5.3.2 Precipitation gradient

As for Prec, its relationship with elevation helps in providing a realistic assessment of water resources and hydrological modeling of mountainous regions (Barros et al., 2004). In recent years, the spatial variability of Prec has received attention because the mass losses of the Himalayan glaciers can be explained with an increased variability in the monsoon system (e.g., Yao et al., 2012; Thakuri et al., 2014). Some previous studies of the Himalayas have considered orographic effects on Prec (Singh and Kumar, 1997; Ichiyanagi et al., 2007). Ichiyanagi et al. (2007), using all available Prec stations operated by DHM, of which < 5% of stations are located over 2500 m and just one station is over 4000 m a.s.l., observed that in the CH-S region, the annual Prec increases with altitude below 2000 m a.s.l. and decreases for elevations ranging between 2000 and 3500 m a.s.l., but with no significant gradient. A broad picture of the relationship between Prec and topography in the Himalayas can be derived from the precipitation radar onboard the Tropical Rainfall Measuring Mission (TRMM). Some authors found an increasing trend with elevation characterized by two distinct maxima along two elevation bands (950 and 2100 m a.s.l.). The second maximum is much higher than the first, and it is located along the Lesser Himalayas. Over these elevations, the annual distribution follows an approximate exponentially decreasing trend (Bookhagen and Burbank, 2006).

Figure 5b shows the altitudinal gradient for the total annual Prec in the Koshi Basin. We observe a clear rise in Prec with elevation until approximately 2500 m a.s.l., corresponding to the Tarke Ghyang station (code 1058), registering an annual mean of 3669 mm (mean for the 2004-2012 period). A linear approximation ($r = 0.83$, $p < 0.001$) provides a rate of +1.16 mm m^{-1}. At higher elevations, we observe an exponential decrease (ae^{bx}, with $a = 21168$ mm m^{-1} and $b = -9\ 10^{-4}$ m^{-1}, where x is the elevation expressed as m a.s.l.) until observing a minimum of 132 mm (years 2009 and 2013) for the Kala Patthar station (AWS4) at 5600 m a.s.l., although, as specified above, at these altitudes the contribution of winter snowfall could be underestimated. The changing point between the two gradients can be reasonably assumed at approximately 2500 m a.s.l., considering that the stations here present the highest interannual variability, belonging in this way, depending on the year, to the linear increase or to the exponential decrease. The clear outlier along the linear gradient is the Num Station (1301) located at 1497 m a.s.l., which recorded 4608 mm of precipitation. This station has been excluded for the linear approximation because, as reported by Montgomery and Stolar (2006), the station is located in the Arun Valley, which acts as a conduit for northward transport of monsoonal precipitation. The result is that local precipitation within the gorge of the Arun River is several times greater than in surrounding areas.

5.4 Spatial distribution of air temperature and precipitation trends in the Koshi Basin

Figure 6 presents the spatial distribution of the Sen's slopes in the Koshi Basin for minT (Fig. 6a), maxT (Fig. 6b), meanT (Fig. 6c), and Prec (Fig. 6d) during the 1994-2013 period. The relevant data are reported in Table 2. The Chainpur (East) station shows T trends in contrast with the other stations (see also Table 2); therefore, we consider this station as a local anomaly and do not discuss it further in the following sections.

In regards to minT, we observe an overall stationary condition in KO-S, as noted above. The only two stations showing a significant increasing trend are both located at East. The high elevation stations (PYRAMID and both those located on the north ridge) differ from the general pattern of the southern basin by showing a significant increasing trend. Even for maxT, we observe a higher increase in the southeastern basin. The central and western parts of the KO-S seem to be more stationary. PYRAMID follows this stationary pattern, while the northern stations (KO-N) show large and significant increases. As a consequence, meanT shows increasing trends for all the Koshi Basin, especially on the southeast and northern sides.

The decrease of precipitation in the southern Koshi Basin presents a quite homogeneous pattern from which the highly elevated PYRAMID is not excluded. The pattern is different on the north ridge, where it is stationary.

6 Discussion

6.1 Temperature trends of the Koshi Basin compared to the regional pattern

Kattel and Yao (2013) analyzed the annual minT, maxT, and meanT trends from stations ranging from 1304 m to 2566 m a.s.l. in CH-S (corresponding to all stations in Nepal) during the 1980–2009 period. They found that the magnitude of warming is higher for maxT (0.065 °C a^{-1}), while minT (0.011 °C a^{-1}) exhibits larger variability, such as positive, negative or no change; meanT was found to increase at an intermediate rate of 0.038 °C a^{-1}. These authors extended some time series and confirmed the findings of Shrestha et al. (1999) that, analyzing the 1971-1994 period, found a maxT increase of 0.059 °C a^{-1} for all of Nepal. Furthermore, warming in the winter was more pronounced compared to other seasons in both studies. These results are consistent with the pattern reported in WH (e.g., Bhutiyani et al., 2007; Shekhar et al., 2010), in EH, and in the rest of India (e.g., Pal and Al-Tabbaa, 2010) for the last three decades.

The trend analysis carried out in this study for the last two decades in KO-S shows full consistency with the pattern of change occurring in these regions over the last three decades in terms of a higher increase in maxT (0.060 °C a^{-1}) than in minT (0.003 °C a^{-1}), a seasonal pattern (more pronounced during the pre- and post-monsoon months), and the magnitudes of the trends (e.g., the meanT trend is +0.030 °C a^{-1}). Therefore, at low elevations of KO-S, we observe an acceleration of warming in the recent years com-

pared to the rate of change reported by Kattel and Yao (2013) and Shrestha et al. (1999) in the previous decades.

Different conditions have been observed on the TP, where the warming of minT is more prominent than that of maxT (e.g., Liu et al., 2006; Liu et al., 2009). In particular, for stations above 2000 m a.s.l. during the 1961–2003 period, Liu et al. (2006) found that minT trends were consistently greater (+0.041 °C a^{-1}) than those of maxT (+0.018 °C a^{-1}), especially in the winter and spring months. Yang et al. (2012), focusing their analysis on CH-N (which corresponds to the southern TP) in a more recent period (1971–2007), showed a significant increase of 0.031 °C a^{-1} for meanT. Yang et al. (2006) analyzed five stations located in a more limited area of CH-N: the northern side of Mt. Everest (therefore, including the two stations also considered in this study) from 1971 to 2004. The warming is observed to be influenced more markedly by the minT increase.

The trend analysis carried out in this study for KO-N over the last two decades agrees with these studies in regards to both the considerable increase of minT (0.034 °C a^{-1}) and the seasonal consistency of trends, related to all three T variables, outside the monsoon months. However, we observe that in recent years, maxT is increasing more than the rest of the TP (0.039 °C a^{-1}). In general we observed an increase of meanT (0.037 °C a^{-1}) comparable to that reported by Yang et al. (2012) (0.031 °C a^{-1}) in the 1971–2007 period.

With all these regional studies, PYRAMID shares the higher T trends outside the monsoon period. However, in contrast with studies located south of the Himalayan ridge, which observed a prevalence of maxT increase, PYRAMID experienced a consistent minT increase (0.072 °C a^{-1} for PYRAMID vs 0.003 °C a^{-1} for KO-S stations), while the maxT increase is decidedly weaker (0.009 °C a^{-1} for PYRAMID vs 0.060 °C a^{-1} for KO-S stations). The remarkable minT trend of PYRAMID is higher, but more similar to the pattern of change commonly described on the TP, in particular in CH-N, and also in this study (0.072 °C a^{-1} for PYRAMID vs 0.034 °C a^{-1} for KO-N stations), while the maxT increase is weaker (0.009 °C a^{-1} for PYRAMID vs 0.039 °C a^{-1} for KO-N stations).

6.2 Elevation dependency of temperature trends

Figure 7 shows T trends in the KO Basin for minT, meanT, and maxT relative to the elevation during the 1994-2013 period. No linear pattern emerges. However, we can observe the minT trend of the three stations located at higher altitude (PYRAMID and KO-N stations), which increases more than that of the lower stations (Fig. 7a, see also Table 2). Reviewing the most recent studies in the surroundings, we found that they are quite exclusively located on CH-N. These studies often show contradictory elevation dependencies (Rangwala and Miller, 2012). A recent study by You et al. (2010) did not find any significant elevation dependency in the warming rates of meanT between 1961 and 2005. However, considering mostly the same stations, Liu et al. (2009) found that

the warming rates for minT were greater at higher elevations. Observations from CH-S are much rarer. Shrestha et al. (1999) found elevation dependency in the rate at which maxT were increasing in the Nepali Himalayas (CH-S), with higher rates at higher elevations, but this study exclusively considered stations under 3000 m a.s.l.

Furthermore we did not find for the Koshi Basin any significant elevation dependency in the weakening rates of Prec.

6.3 Precipitation trends of the Koshi Basin compared to the regional pattern

Turner and Annamalai (2012), using the all-India rainfall data based on a weighted mean of 306 stations, observed a negative precipitation trend since the 1950s in South Asia. According to Yao et al. (2012), using the Global Precipitation Climatology Project (GPCP) data, there is strong evidence that precipitation from 1979 to 2010 decreased even in the Himalayas. In eastern CH-S, where the Koshi Basin is located, they estimated a loss of 173 mm, showing a real decreasing trend starting from the early 1990s (mean value between grid 9 and 11 in Fig. S18 of their paper).

On the TP, the observed pattern of change is opposite that of the monsoon weakening described by the authors cited above. Liu et al. (2010) described an increase in precipitation in CH-N for the period of the 1980s to 2008. Su et al. (2006) described a marked precipitation increase in the Yangtze River Basin (eastern CH-N). In a similar way to the T analysis, Yang et al. (2006) considered 5 stations located on the northern side of Mt. Everest (therefore, including the two stations also considered in this study) from 1971 to 2004 and observed an increasing, but not significant Prec trend. The higher stationarity we observed is confirmed since 1971 for the two KO-N stations considered in this study.

Different from the north side of Mt. Everest and from the general TP, we confirm the general monsoon weakening in the KO-S, observing a substantial Prec decrease of 15% (-11.1 mm a^{-1}, 222 mm), but that is not significant for all stations. At PYRAMID, the annual loss is relatively comparable with that of the KO-S (13.7 mm a^{-1}, 273 mm), but at these high elevations, as we observed in Table 2, the weather is much more drier (449 and 1527 mm, respectively). Therefore, the fractional loss is more than 3 times (52%) that of the KO-S. Considering that the decreasing trend observed during the summer is more robust than the annual one (see above), the fractional loss of Prec during the monsoon is 47%, which means that currently, on average, the precipitation at PYRAMID is the half of what it was twenty years ago.

6.4 Mechanisms responsible for temperature warming and precipitation weakening

According to Rangwala and Miller (2012), there are a number of mechanisms that can cause enhanced warming rates at high elevation, and they often have strong seasonal dependency. These mechanisms arise from either elevation based differential changes in climate drivers, such as snow cover, clouds, specific humidity, aerosols, and soil moisture, or differential sensitivities of surface warming to changes in these drivers

509 at different elevations. This study does not aim to either realize a comprehensive review
510 or to demonstrate the causes that could have led to the climate change pattern observed
511 at PYRAMID, but our intent here is just to note the recent hypotheses advanced in the
512 literature that fit with our observations for the region of investigation.
513 Snow/ice albedo is one of the strongest feedbacks in the climate system (Rangwala
514 and Miller, 2012). Increases in minT are possible if decreases in snow cover are
515 accompanied by increases in soil moisture and surface humidity, which can facilitate a
516 greater diurnal retention of the daytime solar energy in the land surface and amplify the
517 longwave heating of the land surface at night (Rangwala et al., 2012). For the Tibetan
518 Plateau, Rikiishi and Nakasato (2006) found that the length of the snow cover season
519 declined at all elevations between 1966 and 2001. Moreover, minT can be enhanced by
520 nighttime increases in cloud cover. However, assessing changes in clouds and
521 quantifying cloud feedbacks will remain challenging in the near term. For the Tibetan
522 Plateau, Duan and Wu (2006) found that low level nocturnal cloud cover increased over
523 the TP between 1961 and 2003 and that these increases explain part of the observed
524 increases in minT.
525 The maxT increase observed here during April ($p < 0.05$ in 2011, Fig. 4b) fits with
526 the warming reported by Pal and Al-Tabbaa (2010) which observed that within the pre-
527 monsoon season only April shows significant changes in maxT in all Indian regions and
528 WH (1901-2003 period). According to Ramanathan et al. (2007), Gautam et al. (2010)
529 argued that the observed warming during the pre-monsoon period (April-June) can be
530 ascribed not only to the global greenhouse warming, but also to the solar radiation ab-
531 sorption caused by the large amount of aerosol (mineral dust mixed with other carbona-
532 ceous material) transported over the Gangetic-Himalayan region. As recently reported
533 by Marinoni et al. (2013), April represents the month for which the transport of absorb-
534 ing carbonaceous aerosol (i.e. black carbon) is maximized in our region of investigation
535 (Khumbu Valley). At this regards Putero et al. (2013) show evidences for a possible in-
536 fluence of open fire occurrence in South Asia particular abundant during this period of
537 the year. However the significant decreasing of maxT observed in May ($p < 0.05$) and
538 the slight significant decreasing during the monsoon months from June to August ($p <$
539 0.10) appear to deviate from the scenario proposed for April. In this respect it should be
540 kept in mind that the radioactive dynamical interactions of aerosol with the monsoon
541 cycle are extremely complex and different processes can interact with each other. As an
542 instance, as reported by Qian et al. (2011), the deposition of absorbing aerosol on snow
543 and the snow albedo feedback processes can play a prominent role in Himalayas and TP
544 inducing large radioactive flux changes and surface temperature perturbation.
545 Recent studies associate the precipitation decrease over India during the second half
546 of 20th century (e.g., Ramanathan et al., 2005; Lau and Kim, 2006) to the significant
547 tropospheric warming over the tropical area from the Indian Ocean to the western
548 Pacific (e.g., Wu, 2005), while westerlies are strengthening (Zhao et al., 2012). Other
549 authors (e.g., Bollasina et al., 2011) attribute the monsoon weakening to human-
550 influenced aerosol emissions. In fact an increase of aerosols over South Asia has been

well documented (Ramanathan et al., 2005; Lau and Kim, 2006) and climate model experiments suggest that sulfate aerosol may significantly reduce monsoon precipitation (Mitchell and Johns, 1997). Despite a historical weakening of the monsoon circulation, most studies project an increase of the seasonal monsoon rainfall under global warming. At this regards Levy II et al., 2013 find that the dramatic emission reductions (35%–80%) in anthropogenic aerosols and their precursors projected by Representative Concentration Pathway (RCP) 4.5 (Moss et al., 2010) result an increasing trend by the second half of the 21st century in South Asia and in particular over the Himalaya (Palazzi et al., 2013).

6.5 Linking climate change patterns observed at high elevation with glacier responses

6.5.1 Impact of temperature increase

Air temperature and precipitation are the two factors most commonly related to glacier fluctuations. However, there still exists a seasonal gap in order to explain the shrinking of summer accumulation-type glaciers (typical of CH) due to large temperature increases observed in the region during winter (Ueno and Aryal, 2008), as is the case for the south slopes of Mt. Everest. Furthermore, in this study we noted a slightly significant decline in summer maxT and stationary meanT. The real increase of T has been observed for minT, but given the mean elevation of glaciers (5695 m a.s.l. in 1992) and the mean elevation range of glacier fronts (4568-4817 m a.s.l. in 1992, mean 4817 m a.s.l., 249 m of standard deviation –sd-) (Thakuri et al., 2014), this increase for minT can be most likely considered ineffective for melting processes, since T is still less than 0 °C. This inference can be ascertained analyzing Figure 8, created in order to link temperature increases and altitudinal glacier distribution (data from Thakuri et al., 2014). The 0 °C isotherms, corresponding to the mean monthly minT and maxT, are plotted for 1994 and 2013. The elevation of each 0 °C isotherm is calculated according to the accurate lapse rates computation carried out in this study and the observed monthly T trends. We can note that in 1994 the 0 °C isotherm for minT reached the elevation band characterizing the glacier fronts only from June to September. However, twenty years later, the upward of the 0 °C isotherm is modest (92 m) during these months, compared to the huge but ineffective rise for melting processes (downstream from the glacier fronts) of December-November (even 854 m). The maxT has obviously a greater potential impact on glaciers. In fact the 0 °C isotherm for of all months except January and February crosses the elevation bands within which the glacier fronts are located ever since 1994. In this regard we observe that only April (24 m), December (212 m), and November (160 m) experienced an upward of the 0 °C isotherm able to enhance the melting processes, but only close to the glaciers fronts. We therefore point out that the impact caused by the increased temperature occurring in April most likely plays an important role not only in relation to this case study, but also at the level of the Himalayan range. In fact, as mentioned above, Pal and Al-Tabbaa (2010), observed that within the pre-monsoon season, only April showed significant changes in maxT in all

591 Indian regions and WH (1901-2003 period).

592 *6.5.2 Impact of precipitation decrease*
593
594 As regards the precipitation, in this study we noted a strong and significant
595 decreasing Prec trend for all months, corresponding to a fractional loss of 47% during
596 the monsoon season which indicates that, on average, the precipitation at PYRAMID is
597 currently half of what it was twenty years ago. This climate change pattern confirms and
598 clarifies the observation of Thakuri et al. (2014), who noted that the southern Mt.
599 Everest glaciers experienced a shrinkage acceleration over the last twenty years (1992-
600 2011), as underlined by an upward shift of SLA with a velocity almost three times
601 greater than the previous period (1962-1992). The authors, without the support of
602 climatic data, proposed the hypothesis that Mt. Everest glaciers are shrinking faster
603 since the early 1990s mainly as a result of a weakening of precipitation over the last
604 decades. In fact they observed a double upward shift in the SLA of the largest glaciers
605 (south-oriented and with a higher altitude accumulation zone): a clear signal of a
606 significant decrease in accumulation. Wagnon et al. (2013) have recently reached the
607 same conclusion, but also in this case without the support of any climatic studies. Bolch
608 et al. (2011) and Nuimura et al. (2012) registered a higher mass loss rate during the last
609 decade (2000–2010).
610 Furthermore Quincey et al. (2009) and Peters et al. (2010) observed lower glacier
611 flow velocity in the region over the last decades. Many studies highlight how the
612 present condition of ice stagnation of glaciers in the Mt Everest region, and in general
613 in CH-S, is attributable to low flow velocity generated by generally negative mass
614 balances (Bolch et al., 2008; Quincey et al., 2009; Scherler et al., 2011). Our
615 observations allow attributing the lower glacier flow velocity to lower accumulation due
616 to weaker precipitation, which can thus be considered the main climatic factor driving
617 the current ice stagnation of tongues. In this regard we need to keep in mind that
618 changes in velocity are among the main triggers for the formation of supraglacial and
619 proglacial lakes (Salerno et al., 2012; Quincey et al., 2009), which we know to be
620 susceptible to GLOFs.

621 *6.5.3 Trend analysis of annual probability of snowfall*

622 Figure 9 analyses how the changes observed for the meanT at PYRAMID have
623 affected the probability of snowfall on total cumulated annual precipitation in the last
624 twenty years. The increase of meanT observed outside the monsoon period, when the
625 precipitation is almost completely composed by snow (Fig. 2), brought a significant
626 decrease of solid phase (0.7 % a^{-1}, $p < 0.05$). Extending this analysis to the elevation
627 bands characterizing the glaciers distribution (see Fig. 8), through the temperature lapse
628 rate calculated here, we observe that at the level of the mean glaciers (5695 m a.s.l.) the
629 probability of snowfall is stationary (+0.04 % a^{-1}), while it decreases at the mean
630 elevation of SLAs (5345 m a.s.l. in 1992, Thakuri et al., 2014), but not significantly (-

631 0.38 % a^{-1}, $p > 0.1$). The reduction becomes significant at lower altitudes. In particular,
632 at the mean elevation of glacier fronts (4817 m a.s.l.) the probability of snowfall is -0.56
633 % a^{-1} ($p < 0.05$), i.e. at these altitudes the probability of snow on annual base is currently
634 11 % ($p < 0.05$) less than twenty years ago. We can conclude this analysis summarizing
635 that a significant change in precipitation phase has occurred close to the terminal
636 portions of glaciers, corresponding broadly to the glaciers ablation zones (around 10 %,
637 $p < 0.5$), while the lower temperature of the upper glaciers zones has so far guaranteed a
638 stationary condition.

639 **Conclusion**

640 Most relevant studies on temperature trends were conducted on the Tibetan Plateau,
641 the Indian subcontinent (including the WH) and the Upper Indus Basin, while studies
642 on the mountainous regions along the southern slope of the central Himalayas in Nepal
643 (CH-S) are limited. Although Shrestha et al. (1999) analyzed the maximum temperature
644 trends over Nepal during the period 1971–1994, studies on recent temperature trends
645 over CH-S are still lacking and, before this study, completely absent as regards high
646 elevation. This paper addresses seasonal variability of minimum, maximum, and mean
647 temperatures and precipitation at high elevation onthe southern slopes of Mt. Everest.
648 Moreover, we complete this analysis with data from all the existing weather stations
649 located on both sides of the Himalayan range (Koshi Basin) for the 1994-2013 period,
650 during which a rapider glacier mass loss occurred.

651 At high elevation on the southern slopes of Mt. Everest, we observed the following:

652 1) The main increases in air temperature are almost completely concentrated during
653 the post-monsoon months. The pre-monsoon period experienced a slighter and
654 insignificant increase, while the monsoon season is generally stationary. This
655 seasonal temperature change pattern is shared with the entire Koshi Basin, and it
656 is also observed in the regional studies related to the northern and southern
657 slopes of the Himalayan range. Surprisingly, at high elevation the maximum
658 temperature decreases significantly in May and slightly during the monsoon
659 months from June to August.

660 2) The minimum temperature increased much more than the maximum
661 temperature. This remarkable minimum temperature trend is more similar to the
662 pattern of change commonly described on the Tibetan Plateau and confirmed in
663 this study in the northern Koshi Basin. However, this trend is in contrast with
664 studies located south of the Himalayan ridge. As proved by this study, the
665 southern Koshi Basin experienced a prevalence of maximum temperature
666 increases. No linear pattern emerges in the elevation dependency of temperature
667 trends. We only observed higher minimum temperature trends at higher
668 altitudes.

669 3) The total annual precipitation has considerably decreased. The annual rate of
670 decrease at high elevation is similar to the one at lower altitudes on the southern

side of the Koshi Basin, but the drier conditions of this remote environment make the fractional loss relatively more consistent. The precipitation at high elevation during the monsoon period is currently half of what it was twenty years ago. These observations confirm the monsoon weakening observed by previous studies in India and even in the Himalayas since the early 1980s. As opposed to the northern side of the Koshi Basin that shows in this study certain stability, as positive or stationary trends have been observed by previous studies on the TP and more specifically in northern central Himalaya.

4) There is a significantly lower probability of snowfall in the glaciers ablation zones, while the lower temperature of the upper glaciers zones have so far guaranteed a stationary condition.

In general, this study contributes to change the perspective on how the climatic driver (temperature vs. precipitation) led the glacier responses in the last twenty years. to a change perspective related to the climatic driver (temperature vs. precipitation) led the glacier responses in the last twenty years.

Without demonstrating the causes that could have led to the climate change pattern observed at the PYRAMID, we simply note the recent literature on hypotheses that accord with our observations. for the case study.

In conclusion, we have here observed that weather stations at low elevations are not able to suitably describe the climate changes occurring at high altitudes and thus correctly interpret the impact observed on the cryosphere. This consideration stresses the great importance of long-term ground measurements at high elevation.

Author contributions

G.T., Y.M. and E.V. designed research; F.S. performed research; F.S., N.G., S.T., G.V. and E.R. analyzed data; F.S., N.G., E.R. and G.T. wrote the paper. P.C., P.S., N.G. and G.A. data quality check.

Acknowledgements

This work was supported by the MIUR through Ev-K2-CNR/SHARE and CNR-DTA/NEXTDATA project within the framework of the Ev-K2-CNR and Nepal Academy of Science and Technology (NAST). Sudeep Thakuri is recipient of the IPCC Scholarship Award under the collaboration between the IPCC Scholarship Programme and the Prince Albert II of Monaco Foundation's Young Researchers Scholarships Initiative.

References

Fujita, K., and Sakai, A.: Modelling runoff from a Himalayan debris-covered glacier, Hydrol. Earth Syst. Sci., 18, 2679–2694, doi:10.5194/hess-18-2679-2014, 2014.

Ueno, K., Endoh, N., Ohata, T., Yabuki, H., Koike, M., and Zhang, Y.: Characteristics of

precipitation distribution in Tangula, Monsoon, 1993, Bulletin of Glaciological Research, 12, 39-46, 1994.

Abebe, A., Solomatine, D., and Venneker, R.: Application of adaptive fuzzy rule based models for reconstruction of missing precipitation events, Hydrolog. Sci. J., 45, 425–436, doi:10.1080/02626660009492339, 2000.

Abudu, S., Bawazir, A. S., and King, J. P.: Infilling missing daily evapotranspiration data using neural networks, J. Irrig. Drain. E-asce, 136, 317–325, doi:10.1061/(ASCE)IR.1943-4774.0000197, 2010.

Amatya, L. K., Cuccillato, E., Haack, B., Shadie, P., Sattar, N., Bajracharya, B., Shrestha, B. Caroli, P., Panzeri, D., Basani, M., Schommer, B., Flury, B. Salerno, F., and Manfredi, E. C.: Improving communication for management of social-ecological systems in high mountain areas: Development of methodologies and tools – The HKKH Partnership Project, Mt. Res. Dev., 30, 69-79, doi:10.1659/MRD-JOURNAL-D-09-00084.1, 2010.

Bajracharya B., Uddin, K., Chettri, N., Shrestha, B., and Siddiqui, S. A.: Understanding land cover change using a harmonized classification system in the Himalayas: A case study from Sagarmatha National Park, Nepal, Mt. Res. Dev., 30, 143–156, doi: 10.1659/MRD-JOURNAL-D-09-00044.1, 2010.

Barros, A. P., Kim, G., Williams, E., and Nesbitt, S .W.: Probing orographic controls in the Himalayas during the monsoon using satellite imagery, Nat. Hazards Earth Syst. Sci. 4, 29–51, doi:10.5194/nhess-4-29-2004, 2004.

Benn, D. I., Bolch, T., Hands, K., Gulley, J., Luckman, A., Nicholson, L. I., Quincey, D., Thompson, S., Toumi, R., and Wiseman, S.: Response of debris-covered glaciers in the Mount Everest region to recent warming, and implications for outburst flood hazards, Earth-Sci. Rev., 114, 156–174, doi:10.1016/j.earscirev.2012.03.008, 2012.

Bertolani L., Bollasina, M., and Tartari, G.: Recent biannual variability of meteorological features in the Eastern Highland Himalayas, Geophys. Res. Lett., 27, 2185-2188, doi:10.1029/1999GL011198, 2000.

Bhutiyani, M. R., Kale, V. S., and Pawar, N. J.: Long-term trends in maximum, minimum and mean annual air temperatures across the Northwestern Himalaya during the twentieth century, Climatic Change, 85, 159–177, doi:10.1007/s10584-006-9196-1, 2007.

Bocchiola, D. and Diolaiuti, G.: Evidence of climate change within the Adamello Glacier of Italy, Theor. Appl. Climatol., 100, 351–369, doi:10.1007/s00704-009-0186-x, 2010.

Bolch T., Kulkarni, A., Kääb, A., Huggel, C., Paul, F., Cogley, J. G., Frey, H., Kargel, J. S., Fujita, K., Scheel, M., Bajracharya, S., and Stoffel, M.: The state and fate of Himalayan glaciers, Science, 336, 310-314, doi: 10.1126/science.1215828, 2012.

Bolch T., Buchroithner, M., Pieczonka, T., and Kunert, A.: Planimetric and volumetric glacier changes in the Khumbu Himal, Nepal, since 1962 using Corona, Landsat TM and ASTER data, J. Glaciol., 54, 592–600, doi: 0.3189/002214308786570782, 2008.

749 Bolch T., Pieczonka, T., and Benn, D.I.: Multi-decadal mass loss of glaciers in the
750 Everest area (Nepal Himalaya) derived from stereo imagery, The Cryosphere, 5,
751 349–358, doi:10.5194/tc-5-349-2011, 2011.
752 Bollasina, M. A., Ming, Y., and Ramaswamy, V.: Anthropogenic aerosols and the
753 weakening of the south Asian summer monsoon, Science, 334, 502-505,
754 doi:10.1126/science.1204994, 2011.
755 Bookhagen, B. and Burbank, D. W.: Topography, relief, and TRMM-derived rainfall
756 variations along the Himalaya, Geophys. Res. Lett., 33, L08405,
757 doi:10.1029/2006GL026037, 2006.
758 Carraro, E., Guyennon, N., Hamilton, D., Valsecchi, L., Manfredi, E. C., Viviano, G.,
759 Salerno, F., Tartari, G., and Copetti, D.: Coupling high-resolution measurements to a
760 three-dimensional lake model to assess the spatial and temporal dynamics of the
761 cyanobacterium Planktothrix rubescens in a medium-sized lake, Hydrobiologia, 698
762 (1), 77-95. doi:10.1007/s10750-012-1096-y, 2012.
763 Carraro, E., Guyennon, N., Viviano, G., Manfredi, E. C., Valsecchi, L., Salerno, F.,
764 Tartari, G., and Copetti, D.: Impact of Global and Local Pressures on the Ecology of
765 a Medium-Sized Pre-Alpine Lake, in Models of the Ecological Hierarchy, edited by:
766 Jordan, F., and Jorgensen, S. E., Elsevier B.V., pp. 259-274, doi:10.1016/B978-0-
767 444-59396-2.00016-X, 2012b.
768 Coulibaly, P. and Evora, N.: Comparison of neural network methods for infilling
769 missing daily weather records, J. Hydrol., 341, 27–41,
770 doi:10.1016/j.jhydrol.2007.04.020, 2007.
771 Déqué, M.: Frequency of precipitation and temperature extremes over France in an
772 anthropogenic scenario: model results and statistical correction according to
773 observed values, Global Planet. Change, 57, 16–26,
774 doi:10.1016/j.gloplacha.2006.11.030, 2007.
775 Duan, A. and Wu, G.: Change of cloud amount and the climate warming on the Tibetan
776 Plateau, Geophys. Res. Lett., 33, L22704, doi:10.1029/2006GL027946, 2006.
777 Dytham, C.: Choosing and Using Statistics: A Biologist's Guide, John Wiley & Sons,
778 2011.
779 Fujita, K., Sakai, A., Takenaka, S., Nuimura, T., Surazakov, A. B., Sawagaki, T., and
780 Yamanokuchi T.: Potential flood volume of Himalayan glacial lakes, Nat. Hazards
781 Earth Syst. Sci., 13, 1827–1839, doi:10.5194/nhessd-1-15-2013, 2013.
782 Ganguly, N. D. and Iyer, K. N.: Long-term variations of surface air temperature during
783 summer in India, Int. J. Climatol., 29, 735–746, doi:10.1002/joc.1748, 2009.
784 Gardelle, J., Arnaud, Y., and Berthier, E.: Contrasted evolution of glacial lakes along the
785 Hindu Kush Himalaya mountain range between 1990 and 2009, Global Planet.
786 Change, 75, 47-55, doi:10.1016/j.gloplacha.2010.10.003, 2011.
787 Gautam, R., Hsu, N. C. and Lau, K. M.: Premonsoon aerosol characterization and
788 radiative effects over the Indo-Gangetic plains: implications for regional climate
789 warming, J. Geophys. Res., 115, D17208, doi:10.1029/2010JD013819, 2010.
790 Gerstengarbe, F. W. and Werner, P. C.: Estimation of the beginning and end of recurrent

events within a climate regime, Clim. Res., 11, 97-107, 1999.
Guyennon, N., Romano, E., Portoghese, I., Salerno, F., Calmanti, S., Petrangeli, A. B., Tartari, G., and Copetti, D.: Benefits from using combined dynamical-statistical downscaling approaches – lessons from a case study in the Mediterranean region, Hydrol. Earth Syst. Sc., 17, 705–720, doi:10.5194/hess-17-705-2013, 2013.
Hock, R.: Glacier melt: a review of processes and their modeling, Prog. Phys. Geog., 29, 362-391, doi:10.1191/0309133305pp453ra, 2005.
Ichiyanagi, K., Yamanaka, M. D., Muraji, Y., and Vaidya, B. K.: Precipitation in Nepal between 1987 and 1996, Int. J. Climatol., 27, 1753–1762, doi:10.1002/joc.1492, 2007.
Immerzeel, W. W., Petersen, L., Ragettli, S., and Pellicciotti, F.: The importance of observed gradients of air temperature and precipitation for modeling runoff from a glacierized watershed in the Nepal Himalayas, Water Resour. Res., 50, doi:10.1002/2013WR014506, 2014.
James, A. L. and Oldenburg, C. M.: Linear and Monte Carlo uncertainty analysis for subsurface contaminant transport simulation, Water Resour. Res., 33, 2495–2508, doi:10.1029/97WR01925, 1997.
Kattel, D. B. and Yao, T.: Recent temperature trends at mountain stations on the southern slope of the central Himalayas, J. Earth Syst. Sci., 122, 215–227, doi: 10.1007/s12040-012-0257-8, 2013.
Kendall, M.G.: Rank Correlation Methods, Oxford University Press, New York, 1975.
Kivekas, N., Sun, J., Zhan, M., Kerminen, V. M., Hyvarinen, A., Komppula, M., Viisanen, Y., Hong, N., Zhang, Y., Kulmala, M., Zhang, X. C., Deli-Geer, and Lihavainen, H.: Long term particle size distribution measurements at Mount Waliguan, a high-altitude site in inland China, Atmos. Chem. Phys., 9, 5461–5474, doi:10.5194/acp-9-95461-2009, 2009.
Lami, A., Marchetto, A., Musazzi, S., Salerno, F., Tartari, G., Guilizzoni, P., Rogora, M., and Tartari, G. A.: Chemical and biological response of two small lakes in the Khumbu Valley, Himalayas (Nepal) to short-term variability and climatic change as detected by long-term monitoring and paleolimnological methods, Hydrobiologia, 648, 189-205, doi:10.1007/s10750-010-0262-3, 2010.
Lau, K.-M., and Kim, K.-M.: Observational relationships between aerosol and Asian monsoon rainfall, and circulation, Geophys. Res. Lett., 33, L21810, doi: 10.1029/2006GL027546, 2006.
Lavagnini, I., Badocco, D., Pastore, P., and Magno, F.: Theil-Sen nonparametric regression technique on univariate calibration, inverse regression and detection limits, Talanta, 87, 180-188, doi:10.1016/j.talanta.2011.09.059, 2011.
Levy II, H., L. W., Horowitz, M. D., Schwarzkopf, Y., Ming, J. C., Golaz, V., Naik, and Ramaswamy, V.: The roles of aerosol direct and indirect effects in past and future climate change, J. Geophys. Res., 118, 1–12, doi:10.1002/jgrd.50192, 2013.
Liu, J., Yang, B., and Qin, C.: Tree-ring based annual precipitation reconstruction since AD 1480 in south central Tibet. Quatern. Int., 236, 75-81,

833 doi:10.1016/j.quaint.2010.03.020, 2010.
834 Liu, K., Cheng, Z., Yan, L., and Yin, Z.: Elevation dependency of recent and future min-
835 imum surface air temperature trends in the Tibetan Plateau and its surroundings,
836 Global Planet. Change, 68, 164–174, doi:10.1016/j.gloplacha.2009.03.017, 2009.
837 Liu, X. D., and Chen, B. D.: Climatic warming in the Tibetan Plateau during recent
838 decades, Int. J. Climatol., 20, 1729–1742, doi:10.1002/1097-
839 0088(20001130)20:14<1729::AID-JOC556>3.0.CO;2-Y, 2000.
840 Liu, X.D., Yin, Z. Y., Shao, X., and Qin, N.: Temporal trends and variability of daily
841 maximum and minimum, extreme temperature events, and growing season length
842 over the eastern and central Tibetan Plateau during 1961–2003, J. Geophys. Res.,
843 111, D19, doi:10.1029/2005JD006915, 2006.
844 Manfredi, E. C., Flury, B., Viviano, G., Thakuri, S., Khanal, S. N., Jha, P. K., Maskey,
845 R. K., Kayastha, R. B., Kafle, K. R., Bhochhibhoya, S., Ghimire, N. P., Shrestha, B.
846 B., Chaudhary, G., Giannino, F., Carteni, F., Mazzoleni, S., and Salerno, F.: Solid
847 waste and water quality management models for Sagarmatha National Park and
848 Buffer Zone, Nepal: implementation of a participatory modeling framework, Mt.
849 Res. Dev., 30, 127-142, doi:10.1659/MRD-JOURNAL-D-10-00028.1, 2010.
850 Marinoni, A., Cristofanelli, P., Laj, P., Putero, D., Calzolari, F., Landi, T. C., Vuillermoz,
851 E., Maione, M., and Bonasoni, P.: High black carbon and ozone concentrations
852 during pollution transport in the Himalayas: Five years of continuous observations at
853 NCO-Prec global GAW station, J. Environ. Sci., 25, 1618–1625, doi:10.1016/S1001-
854 0742(12)60242-3, 2013.
855 Mitchell, J. F. B. and Johns, T. C.: On the modification of global warming by sulphate
856 aerosols. J. Climate, 10, 245-267, 1997.
857 Montgomery, D. R. and Stolar, D. B.: Reconsidering Himalayan river anticlines,
858 Geomorphology, 82, 4–15, doi:10.1016/j.geomorph.2005.08.021, 2006.
859 Moss, R. H., et al.: The next generation of scenarios for climate change research and
860 assessment, Nature, 463, 747–756, doi:10.1038/nature08823, 2010.
861 Nuimura, T., Fujita, K., Yamaguchi, S., and Sharma, R. R.: Elevation changes of
862 glaciers revealed by multitemporal digital elevation models calibrated by GPS survey
863 in the Khumbu region, Nepal Himalaya, 1992–2008, J. Glaciol., 58, 648–656, doi:
864 10.3189/2012JoG11J061, 2012.
865 Pal, I. and Al-Tabbaa, A.: Long-term changes and variability of monthly extreme tem-
866 peratures in India, Theor. Appl. Climatol., 100, 45–56, doi:10.1007/s00704-009-
867 0167-0, 2010.
868 Palazzi, E., von Hardenberg, J., and Provenzale, A.: Precipitation in the Hindu-Kush
869 Karakoram Himalaya: Observations and future scenarios, J. Geophys. Res., 118, 85-
870 100, doi: 10.1029/2012JD018697, 2013.
871 Pepin, N. C. and Lundqist, J. D.: Temperature trends at high elevations: patterns across
872 the globe, Geophys. Res. Lett., 35, doi:10.1029/2008GL034026, 2008.
873 Peters, J., Bolch, T., Buchroithner, M. F., and Bäßler, M.: Glacier Surface Velocities in
874 the Mount Everest Area/Nepal using ASTER and Ikonos imagery, Proceeding of 10th

International Symposium on High Mountain Remote Sensing Cartography, Kathmandu, Nepal, 313-320, 2010.
Putero, D., T. C., Landi, P., Cristofanelli, A., Marinoni, P., Laj, R., Duchi, F., Calzolari, G. P., Verza and P. Bonasoni, Influence of open vegetation fires on black carbon and ozone variability in the southern Himalayas (NCO-P, 5079 m a.s.l.), Environ. Pollut., 184, 597-604, doi: 10.1016/j.envpol.2013.09.035, 2013.
Qian, Y., Flanner, M., Leung, L., and Wang, W.: Sensitivity studies on the impacts of Tibetan plateau snowpack pollution on the Asian hydrological cycle and monsoon climate, Atmos. Chem. Phys., 11, 1929–1948, doi:10.5194/acp-11-1929-2011, 2011.
Quincey, D. J., Luckman, A., and Benn, D.: Quantification of Everest region glacier velocities between 1992 and 2002, using satellite radar interferometry and feature tracking, J. Glaciol., 55, 596-606, doi: 10.3189/002214309789470987, 2009.
Ramanathan, V., Chung, C., Kim, D., Bettge, T., Buja, L., Kiehl, J. T., Washington, W. M., Fu, Q., Sikka, D. R., and Wild, M.: Atmospheric brown clouds: Impacts on South Asian climate and hydrological cycle. Proc. Natl. Acad. Sci. U.S.A, 102, 5326- 5333, doi: 10.1073/pnas.0500656102, 2005.
Ramanathan, V., Li, F., Ramana, M. V., Praveen, P. S., Kim, D., Corrigan, C. E., Nguyen, H., Stone, E. A., Schauer, J. J., Carmichael, G. R., Adhikary, B., and Yoon, S. C.: Atmospheric brown clouds: Hemispherical and regional variations in long-range transport, absorbtion, and radiative forcing, J. Geophys. Res., 112, D22, doi:10.1029/2006JD008124, 2007.
Rangwala, I. and Miller, J. R.: Climate change in mountains: a review of elevation-dependent warming and its possible causes, Climatic Change, 114, 527–547, doi:10.1007/s10584-012-0419-3, 2012.
Rangwala, I., Barsugli, J., Cozzetto, K., Neff, J., and Prairie, J.: Mid-21st century projections in temperature extremes in the southern Colorado Rocky Mountains from regional climate models, Clim Dyn., 39, 1823-1840, doi:10.1007/s00382- 011-1282-z, 2012.
Rikiishi, K. and Nakasato, H.: Height dependence of the tendency for reduction in seasonal snow cover in the Himalaya and the Tibetan Plateau region, 1966–2001, Ann. Glaciol., 43, 369–377, doi: http://dx.doi.org/10.3189/172756406781811989, 2006.
Salerno, F., Buraschi, E., Bruccoleri, G., Tartari, G., and Smiraglia, C.: Glacier surface-area changes in Sagarmatha National Park, Nepal, in the second half of the 20th century, by comparison of historical maps, J. Glaciol., 54, 738-752, 2008.
Salerno, F., Viviano, G., Mangredi, E. C., Caroli, P., Thakuri, S., and Tartari, G.: Multiple Carrying Capacities from a management-oriented perspective to operationalize sustainable tourism in protected area, J. Environ. Manage., 128, 116-125, doi:10.1016/j.jenvman.2013.04.043, 2013.
Salerno, F., Gambelli, S., Viviano, G., Thakuri, S., Guyennon, N., D'Agata, C., Diolaiuti, G., Smiraglia, C., Stefani, F., Bochhiola, D., and Tartari, G.: High alpine ponds shift upwards as average temperature increase: A case study of the Ortles-

917 Cevedale mountain group (Southern alps, Italy) over the last 50 years, Global Planet.
918 Change, doi: 10.1016/j.gloplacha.2014.06.003, 2014.
919 Salerno, F., Thakuri, S., D'Agata, C., Smiraglia, C., Manfredi, E. C., Viviano, G., and
920 Tartari, G.: Glacial lake distribution in the Mount Everest region: Uncertainty of
921 measurement and conditions of formation, Global Planet. Change, 92-93, 30-39,
922 doi:10.1016/j.gloplacha.2012.04.001, 2012.
923 Scherler, D., Bookhagen, B., and Strecker, M.R.: Spatially variable response of Himala-
924 yan glaciers to climate change affected by debris cover. Nature Geosci., 4, 156–159,
925 doi:10.1038/ngeo1068, 2011.
926 Schneider, T.: Analysis of incomplete climate data: Estimation of mean values and
927 covariance matrices and imputation of missing values, J. Clim., 14, 853–871,
928 doi:10.1175/1520-0442(2001)014<0853:AOICDE>2.0.CO;2, 2001.
929 Sellegri, K., Laj, P., Venzac, H., Boulon, J., Picard, D., Villani, P., Bonasoni, P.,
930 Marinoni, A., Cristofanelli, P., and Vuillermoz, E.: Seasonal variations of aerosol size
931 distributions based on long-term measurements at the high altitude Himalayan site of
932 Nepal Climate Observatory—Pyramid (5079 m), Nepal, Atmos. Chem. Phys., 10,
933 10679–10690, doi:10.5194/acp-10.10679-2010, 2010.
934 Sen, P. K.: Estimates of the regression coefficient based on Kendall's Tau, J. Am.
935 Assoc., 63, 1379-1389, doi:10.2307/2285891, 1968.
936 Shekhar, M. S., Chand, H., Kumar, S., Srinivasan, K., and Ganju, A.: Climate-change
937 studies in the western Himalaya, Ann. Glaciol., 51, 105-112,
938 doi:10.3189/172756410791386508, 2010.
939 Shrestha, A. B., Wake, C. P., Mayewski, P. A., and Dibb, J. E.: Maximum temperature
940 trends in the Himalaya and its vicinity: An analysis based on temperature records
941 from Nepal for the period 1971-94, J. Clim., 12, 2775-5561, doi:10.1175/1520-
942 0442(1999)012<2775:MTTITH>2.0.CO;2, 1999.
943 Singh, P. and Kumar, N.: Effect of orography on precipitation in the western Himalayan
944 region, J. Hydrol., 199, 183-206, doi:10.1016/S0022-1694(96)03222-2, 1997.
945 Su, B. D., Jiang, T., and Jin, W. B.: Recent trends in observed temperature and
946 precipitation extremes in the Yangtze River basin, China, Theor. Appl. Climatol., 83,
947 139–151, doi:10.1007/s00704-005-0139-y, 2006.
948 Tartari, G., Vuillermoz, E., Manfredi, E. C., and Toffolon, R.: CEOP High Elevations
949 Initiative, GEWEX News, Special Issue, 19(3), 4-5, 2009.
950 Tartari, G., Salerno, F., Buraschi, E., Bruccoleri, G., and Smiraglia, C.: Lake surface
951 area variations in the North-Eastern sector of Sagarmatha National Park (Nepal) at
952 the end of the 20th Century by comparison of historical maps, J. Limnol., 67, 139-
953 154, doi:10.4081/jlimnol.2008.139, 2008.
954 Tartari, G., Verza, P., and Bertolami, L.: Meteorological data at PYRAMID Observatory
955 Laboratory (Khumbu Valley, Sagarmatha National Park, Nepal), in Limnology of
956 high altitude lakes in the Mt. Everest Region (Nepal), edited by: Lami, A. and
957 Giussani, G., Mem. Ist. Ital. Idrobiol, 57, 23-40, 2002.
958 Thakuri, S., Salerno, F., Smiraglia, C., Bolch, T., D'Agata, C., Viviano, G., and Tartari,

959 G.: Tracing glacier changes since the 1960s on the south slope of Mt. Everest (central
960 southern Himalaya) using optical satellite imagery, The Cryosphere, 8, 1297-1315,
961 doi:10.5194/tc-8-1297-2014, 2014.
962 Themeßl, M. J., Gobiet, A., and Heinrich, G.: Empirical-statistical downscaling and
963 error correction of regional climate models and its impact on the climate change
964 signal, Climatic Change, 112, 449-468, doi:10.1007/s10584-011-011-0224-4, 2012.
965 Turner, A. G. and Annamalai, H.: Climate change and the South Asian summer
966 monsoon, Nat. Clim. Change, 2, 587-595, doi:10.1038/nclimate1495, 2012.
967 Ueno K. and Aryal, R.: Impact of tropical convective activity on monthly temperature
968 variability during non monsoon season in the Nepal Himalayas, J. Geophys. Res.,
969 113, D18112, doi:10.1029/2007JD009524, 2008.
970 UNEP (United Nations Environment Programme)/WCMC (World Conservation
971 Monitoring Centre): Sagarmatha National Park, Nepal, in Encyclopedia of Earth,
972 edited by: McGinley, M. and Cleveland, C. J., Environmental Information Coalition,
973 National Council for Science and the Environment, Washington, DC, 2008.
974 Venzac, H., Sellegri, K., Laj, P., Villani, P., Bonasoni, P., Marinoni, A., Cristofanelli, P.,
975 Calzolari, F., Fuzzi, S., Decesari, S., Facchini, M. C., Vullermoz, E., and Verza, G. P.:
976 High frequency new particle formation in the Himalayas, Proc. Natl. Acad. Sci.
977 USA, 105, 15666-15671, doi:10.1073/pnas.0801355105, 2008.
978 Vuille, M.: Climate variability and high altitude temperature and precipitation, in
979 Encyclopedia of snow, ice and glaciers, edited by: Singh, V. P. et al., Springer, pp.
980 153-156, 2011.
981 Wagnon, P., Vincent, C., Arnaud, Y., Berthier, E., Vuillermoz, E., Gruber, S., Ménégoz,
982 M., Gilbert, A., Dumont, M., Shea, J. M., Stumm, D., and Pokhrel, B. P.: Seasonal
983 and annual mass balances of Mera and Pokalde glaciers (Nepal Himalaya) since
984 2007, The Cryosphere, 7, 1769-1786, doi:10.5194/tc-7-1769-2013, 2013.
985 Washington, W. M. and Parkinson, C. L.: An introduction to three-Dimensional Climate
986 Modeling, 2nd Edition, University Science Books, Sausalito, 2005.
987 Wu, B.: Weakening of Indian summer monsoon in recent decades, Adv. Atmos. Sci.
988 22(1), 21-29, doi:10.1007/BF02930866, 2005.
989 Yang J., Tan, C., and Zhang, T.: Spatial and temporal variations in air temperature and
990 precipitation in the Chinese Himalayas during the 1971–2007, Int. J. Climatol., 33,
991 2622-2632, doi:10.1002/joc.3609, 2012.
992 Yang, X., Zhang, Y., Zhang, W., Yan, Y., Wang, Z., Ding, M., and Chu, D.: Climate
993 change in Mt. Qomolangma region since 1971, J. Geogr. Sci., 16, 326-336,
994 doi:10.1007/s11442-006-0308-7, 2006.
995 Yao, T., Thompson, L., Yang, W., Yu, W., Gao, Y., Guo, X., Yang, X., Duan, K., Zhao,
996 H., Xu, B., Pu, J., Lu, A., Xiang, Y., Kattel, D. B., and Joswiak, D.: Different glacier
997 status with atmospheric circulations in Tibetan Plateau and surroundings, Nat. Clim.
998 Change, 2, 663-667, doi:10.1038/nclimate1580, 2012.
999 You, Q., Kang, S., Pepin, N., Flügel, W., Yan, Y., Behrawan, H., and Huang, J.: Rela-
1000 tionship between temperature trend magnitude, elevation and mean temperature in

1001 the Tibetan Plateau from homogenized surface stations and reanalysis data, Global
1002 Planet. Change, 71, 124-133, doi:10.1016/j.gloplacha.2010.01.020, 2010.
1003 Zhao, H., Xu, B., Yao, T., Wu, G., Lin, S., Gao, J., and Wang, M.: Deuterium excess
1004 record in a southern Tibetan ice core and its potential climatic implications, Clim.
1005 Dyn., 38, 1791-1803, doi:10.1007/s00382-011-1161-7, 2012.

1006

1007 *Table 1. List of surface stations belonging to PYRAMID Observatory Laboratory*
1008 *network located along the south slopes of Mt. Everest (upper DK Basin).*

Station ID	Location	Latitude °N	Longitude °E	Elevation m a.s.l.	Sampling Frequency	Data Availability		% of daily missing data	
						From	To	Air Temperature	Precipitation
AWS3	Lukla	27.70	86.72	2660	1 hour	02/11/2004	31/12/2012	23	20
AWSN	Namche	27.80	86.71	3570	1 hour	27/10/2001	31/12/2012	21	27
AWS2	Pheriche	27.90	86.82	4260	1 hour	25/10/2001	31/12/2013	15	22
AWS0	Pyramid	27.96	86.81	5035	2 hours	01/01/1994	31/12/2005	19	16
AWS1	Pyramid	27.96	86.81	5035	1 hour	01/01/2000	31/12/2013	10	21
ABC	Pyramid	27.96	86.82	5079	1 hour	01/03/2006	31/12/2011	5	1
AWS4	Kala Patthar	27.99	86.83	5600	10 minutes	01/01/2009	31/12/2013	28	38
AWS5	South Col	27.96	86.93	7986	10 minutes	01/05/2008	31/10/2011	39	100

1009

1010

*Table 2. List of ground weather stations located in the Koshi Basin and descriptive statistics of the Sen's slopes for minimum, maximum, and mean air temperatures and total precipitation for the 1994-2012 period. The annual mean air temperature, the total annual mean precipitation, and the percentage of missing daily values is also reported. Level of significance (° p-value = 0.1, * p-value = 0.05, ** p-value = 0.01, and *** p-value = 0.001).*

						Air Temperature					Precipitation		
	ID	Station Name	Latitude	Longitude	Elevation	Annual mean	Missing values	MinT trend	MaxT Trend	MeanT trend	Annual total	Missing values	Prec trend
			°N	°N	m a.s.l.	°C	%	°C a^{-1}	°C a^{-1}	°C a^{-1}	mm	%	mm a^{-1}
KO-S (NEPAL)	1024	DHULIKHEL	27.61	85.55	1552	17.1	2	-0.012	0.041	0.026			
	1036	PANCHKHAL	27.68	85.63	865	21.4	10	0.038	0.051 *	0.038 °	1191	10	-25.0 *
	1058	TARKE GHYANG	28.00	85.55	2480						3669	10	-21.9
	1101	NAGDAHA	27.68	86.10	850						1369	3	-1.4
	1103	JIRI	27.63	86.23	2003	14.4	1	0.013	0.020	0.014 °	2484	4	6.6
	1202	CHAURIKHARK	27.70	86.71	2619						2148	2	1.3
	1206	OKHALDHUNGA	27.31	86.50	1720	17.6	2	-0.017	0.042	0.000	1786	3	-5.1
	1210	KURULE GHAT	27.13	86.41	497						1017	2	-23.4 °
	1211	KHOTANG BAZAR	27.03	86.83	1295						1324	4	15.9
	1222	DIKTEL	27.21	86.80	1623						1402	6	10.4
	1301	NUM	27.55	87.28	1497						4537	6	-54.3 **
	1303	CHAINPUR (EAST)	27.28	87.33	1329	19.1	0	-0.127 *	0.024	-0.064 °	1469	0	-1.1
	1304	PAKHRIBAS	27.05	87.28	1680	16.7	0	-0.005	0.036 *	0.015	1540	4	-3.7
	1307	DHANKUTA	26.98	87.35	1210	20.0	0	-0.002	0.153 ***	0.071 ***	942	6	-9.2 °
	1314	TERHATHUM	27.13	87.55	1633	18.2	10	0.033	0.066 °	0.049 *	1052	6	-13.1 °
	1317	CHEPUWA	27.46	87.25	2590						2531	5	-41.9 *
	1322	MACHUWAGHAT	26.96	87.16	158						1429	6	-22.9 °
	1403	LUNGTHUNG	27.55	87.78	1780						2347	1	2.6
	1405	TAPLEJUNG	27.35	87.66	1732	16.6	1	0.060 *	0.085 **	0.071 **	1966	3	-11.6
	1419	PHIDIM	27.15	87.75	1205	21.2	7	0.047 *	0.082 **	0.067 **	1287	2	-13.6 *
		MEAN	**27.33**	**87.00**	**1587**	**17.9**	**2**	**0.003**	**0.060** °	**0.029** °	**1527**	**4**	**-11.1**
		PYRAMID	**27.96**	**86.81**	**5035**	**-2.4**	**0**	**0.072** ***	**0.009**	**0.044** *	**449**	**0**	**-13.7** ***
KO-N (TIBET)		DINGRI	28.63	87.08	4,302	3.5	0	0.037 °	0.041 °	0.037 *	309	0	-0.1
		NYALAM	28.18	85.97	3,811	4.1	0	0.032 °	0.036 °	0.036 °	616	0	-0.2
		MEAN	**28.41**	**86.53**	**4,057**	**3.8**	**0.1**	**0.034** °	**0.039** *	**0.037** *	**463**	**0**	**-0.1**

*Table 3. Descriptive statistics of the Sen's slopes on a seasonal basis for minimum, maximum, and mean air temperatures and total precipitation of weather stations located in the Koshi Basin for the 1994-2012 period. The Nepali and Tibetan stations are aggregated as mean values. Level of significance (° p-value = 0.1, * p-value = 0.05, ** p-value = 0.01, and *** p-value = 0.001). Annual and seasonal temperature trends are expressed as °C a^{-1}. Annual precipitation trend is expressed as mm a^{-1}, while the seasonal precipitation trends are in mm (4 months) a^{-1}.*

Location	Minimum Temperature				Maximum Temperature				Mean Temperature				Total Precipitation			
	Pre-	Monsoon	Post-	Annual	Pre-	Monsoon	Post-	Annual	Pre-	Monsoon	Post-	Annual	Pre-	Monsoon	Post-	Annual
SOUTHER KOSHI BASIN (KO-S, NEPAL)	0.012	-0.005	-0.001	0.003	0.076 °	0.052	0.069 °	0.060 °	0.043	0.020	0.030	0.030 °	0.8	-8.6	-2.5	-11.1
PYRAMID (NEPAL)	0.067 °	0.041 °	0.151 ***	0.072 ***	0.024	-0.028	0.049	0.009	0.035	0.015	0.124 **	0.044 **	-2.5 **	-9.3 **	-1.4 **	-13.7 ***
NORTHERN KOSHI BASIN (KO-N,TIBET)	0.042 °	0.019	0.086 *	0.034 °	0.023	0.030	0.071 *	0.039 °	0.042 °	0.013	0.084 *	0.037 *	2.2	0.4	-3.3 *	-0.1

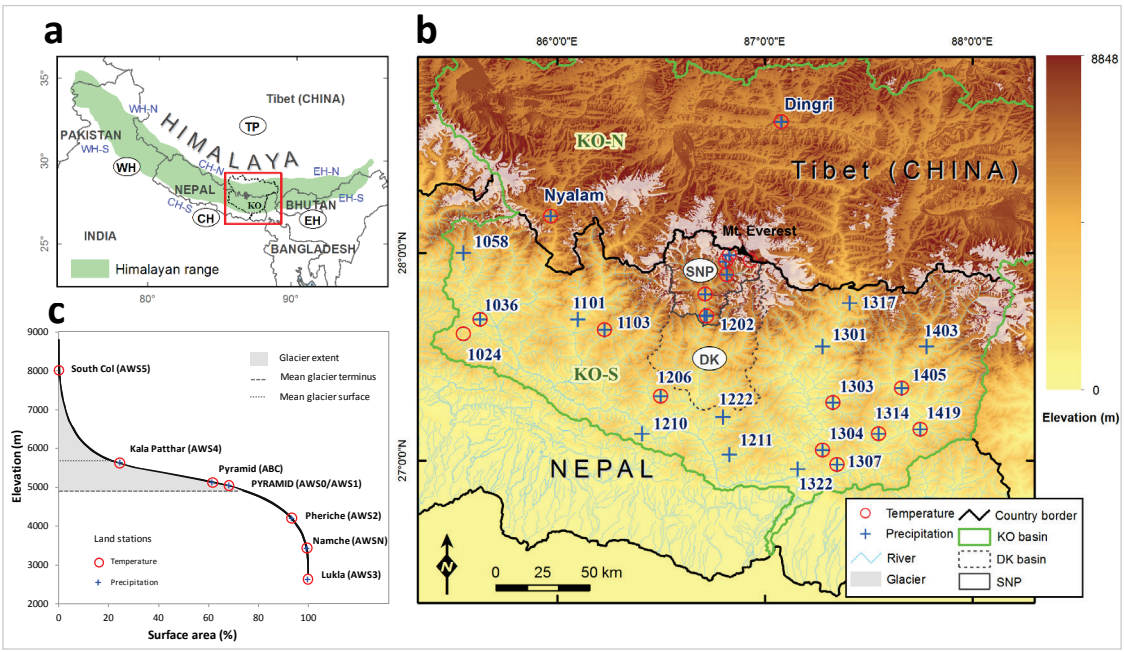

Figure 1. a) Location of the study area in the Himalaya, where the abbreviations WH, CH, EH represents the Western, Central and Eastern Himalaya, respectively (the suffixes -N and -S indicate the northern and southern slopes). b) Focused map on the spatial distribution of all meteorological stations used in this study, where KO and DK stand for the Koshi and Dudh Koshi Basins, respectively; SNP represents the Sagarmatha National Park. c) Hypsometric curve of SNP (upper DK Basin) and altitudinal glacier distribution. Along this curve, the locations of meteorological stations belonging to PYRAMID Observatory Laboratory are presented.

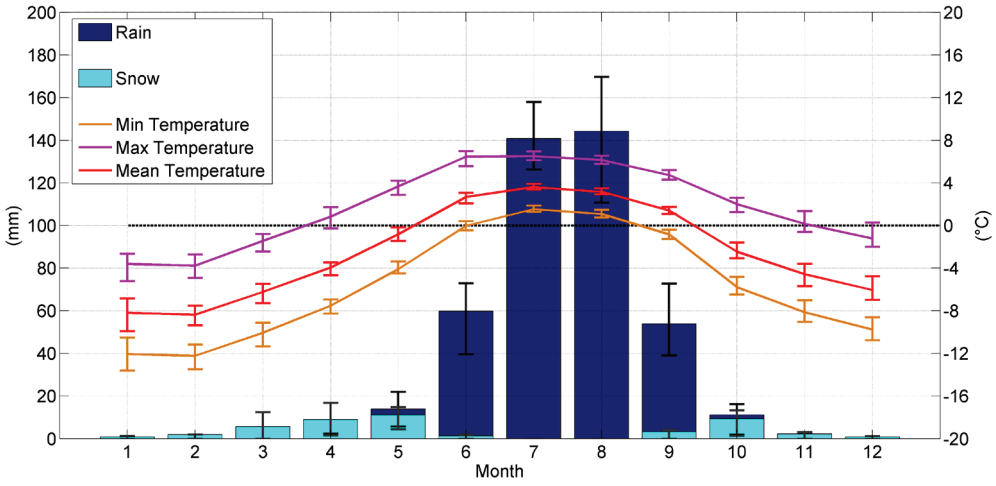

1039

1040 *Figure 2. Mean monthly cumulated precipitation subdivided into snowfall and rainfall*
1041 *and minimum, maximum, and mean temperature at 5050 m a.s.l. (reference period*
1042 *1994-2013). The bars represent the standard deviation.*

1043

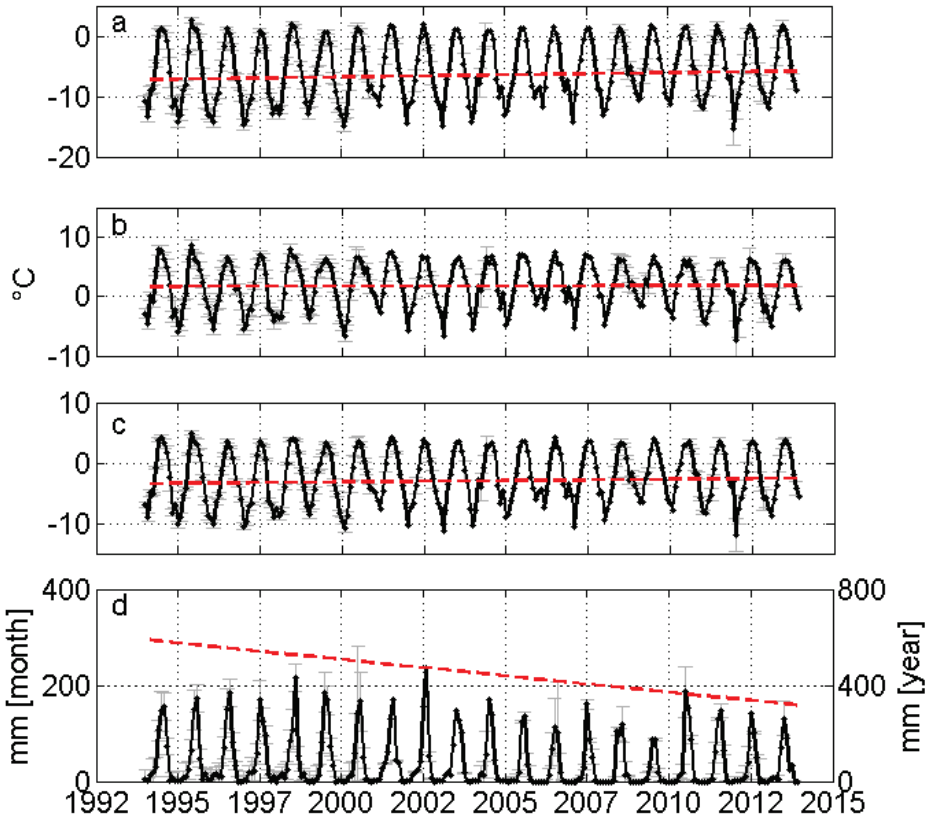

Figure 3. Temperature and precipitation monthly time series (1994-2013) reconstructed at high elevations of Mt. Everest (PYRAMID): minimum (a), maximum (b), and mean temperature (c), and precipitation (d). Uncertainty at 95% is presented as gray bar. The red lines represents the robust linear fitting of the time series characterized by the associated Sen's slope. According to Dytham (2011), the intercepts are calculated by taking the slopes back from every observation to the origin. The intercepts used in here represent the median values of the intercepts calculated for every point (Lavagnini et al., 2011). For precipitation the linear fitting refers at the right axis.

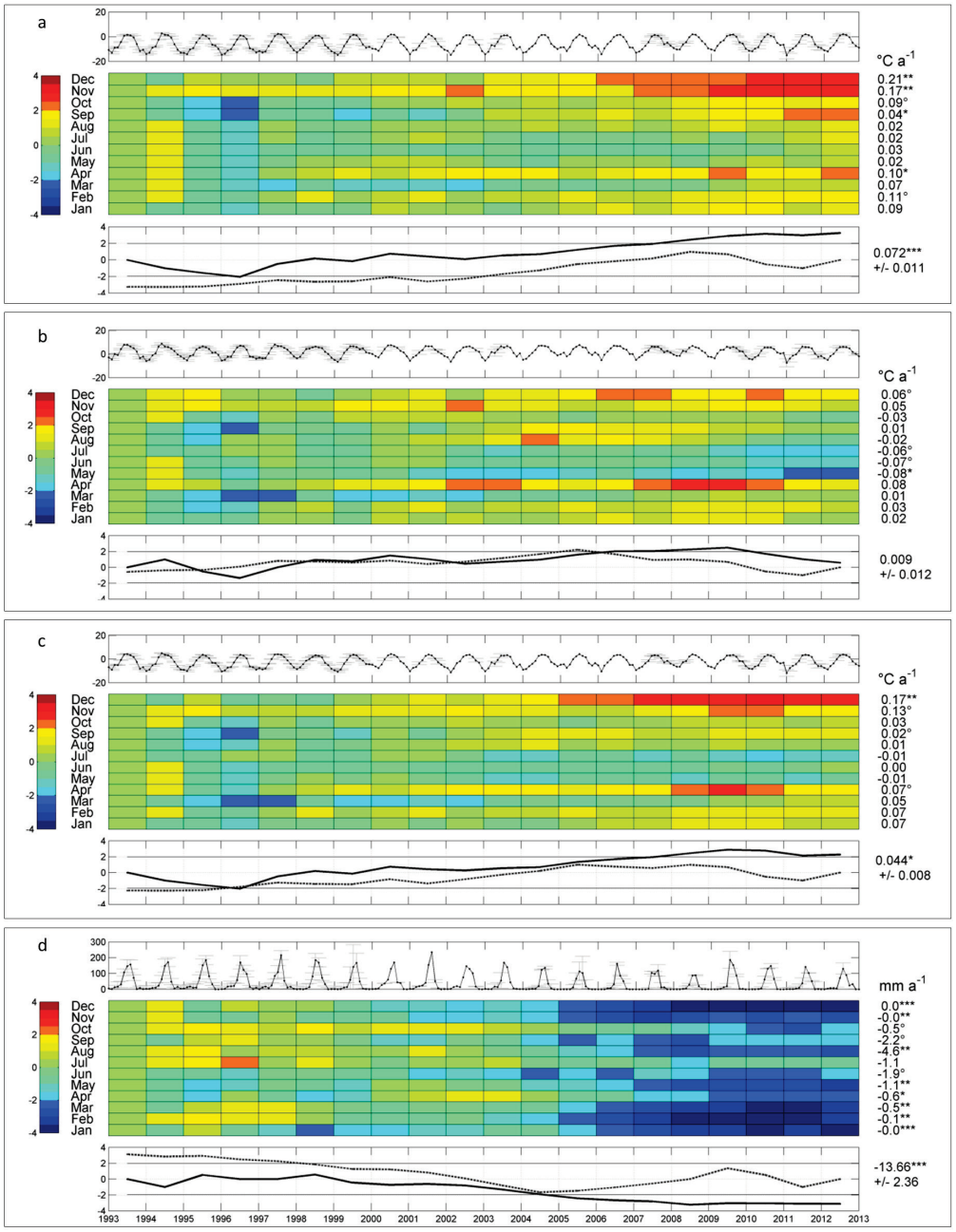

*Figure 4. Trend analysis for a) minimum, b) maximum, and c) mean air temperatures and d) total precipitation in the upper DK Basin. The top graph of each meteorological variable shows the monthly trend (dark line) and uncertainty due to the reconstruction process (gray bars). The central grid displays the results of the sequential Mann-Kendall (seqMK) test applied at the monthly level. On the left, the color bar represents the normalized Kendall's tau coefficient μ(τ). The color tones below –1.96 and above 1.96 are significant (α = 5%). On the right, the monthly Sen's slopes and the relevant significance levels for the 1994-2013 period (° p-value = 0.1, * p-value = 0.05, ** p-value = 0.01, and *** p-value = 0.001). The bottom graph plots the progressive (black line) and retrograde (dotted line) μ(τ) applied on the annual scale. On the right, the annual Sen's slope is shown for the 1994-2013 period.*

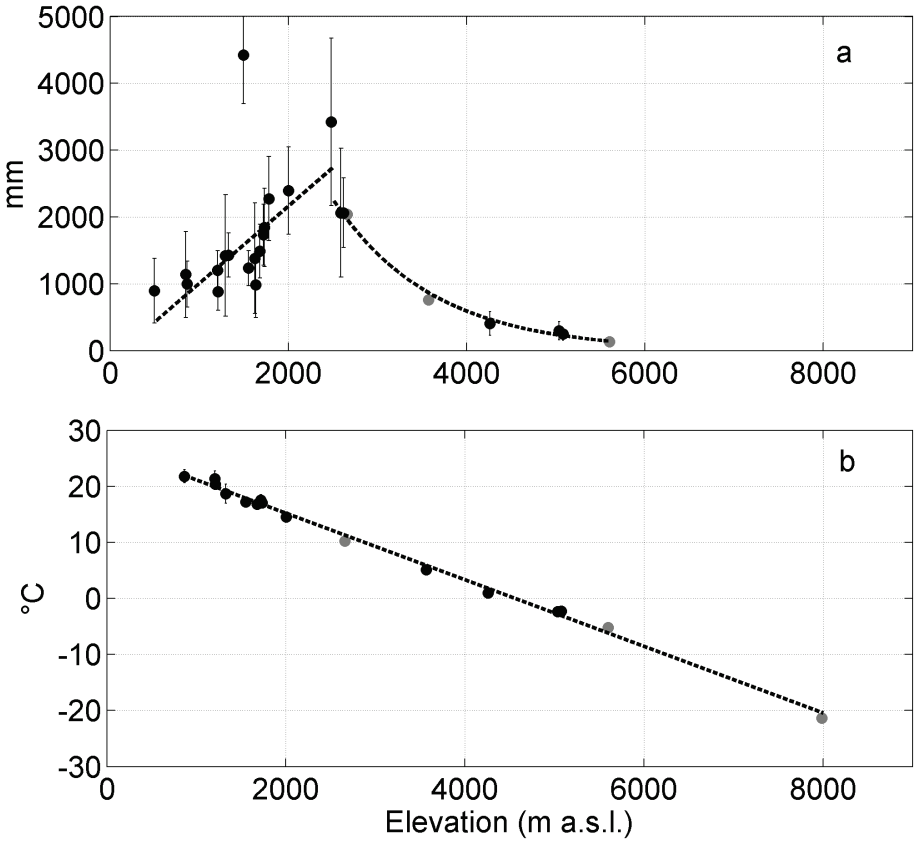

Figure 5. Lapse rates of (a) mean annual air temperature and (b) total annual precipitation in the Koshi Basin for the last 10 years (2003-2012). The daily missing data threshold is set to 10%. Only stations presenting at least 5 years of data (black points) are considered to create the regressions (the bars represent two standard deviations). Gray points indicate the stations presenting less than 5 years of data.

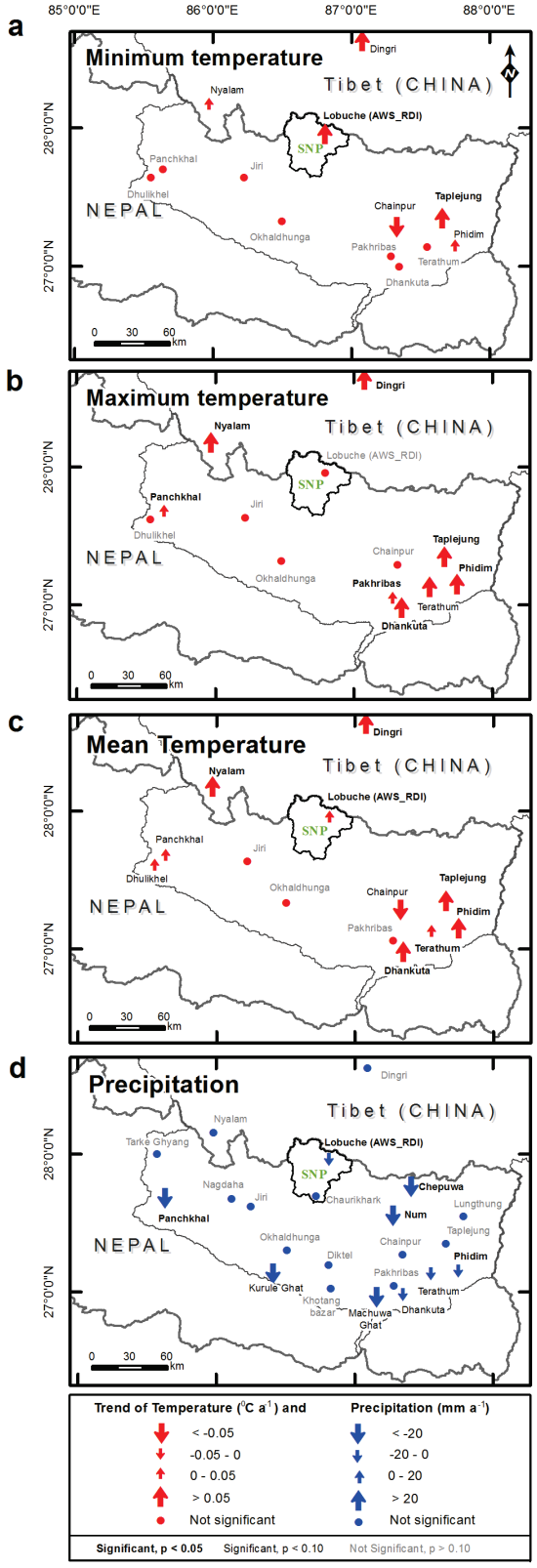

Figure 6. Spatial distribution of the Sen's slopes in the Koshi Basin for minimum (a), maximum (b), and mean (c) air temperature and (d) total precipitation for the 1994-2013 period. Data are reported in Table 2.

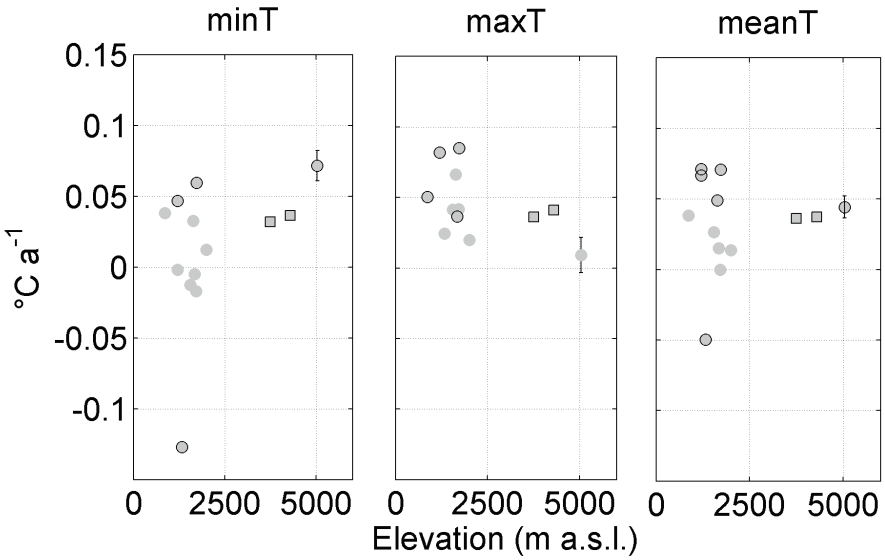

Figure 7. Elevation dependency of minimum (a), maximum (b), and mean (c) air temperatures with the Sen's slopes for the 1994-2013 period. The circle indicates stations with less than 10% of missing daily data, and the star indicates stations showing a trend with p-value < 0.1. The red marker represents the trend and the associated uncertainty (two standard deviations) referred to the reconstructed time series for the AWS1 station (Pyramid). Data are reported in Table 2.

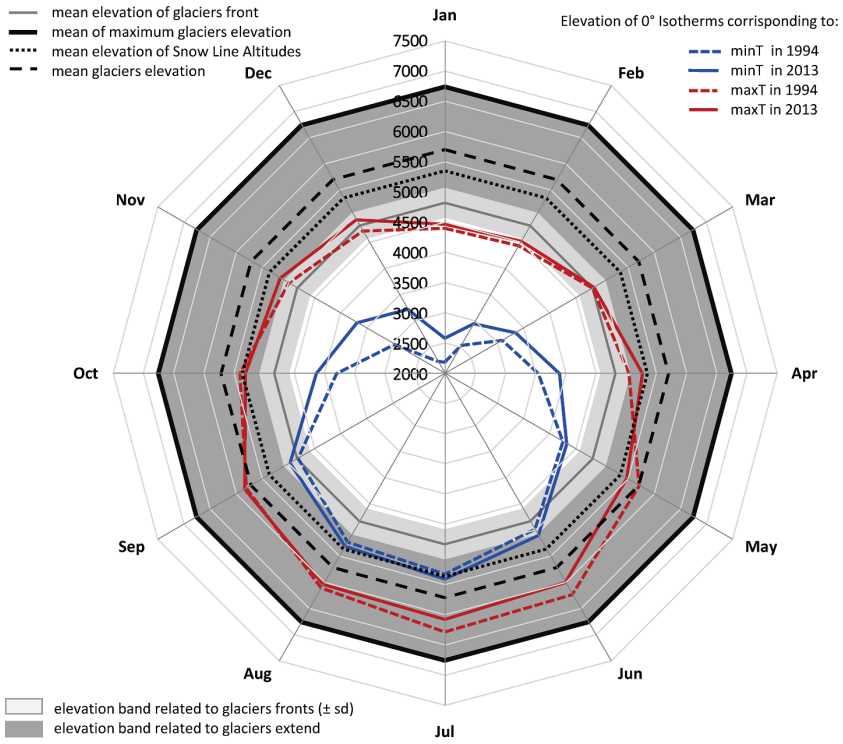

1085

1086 *Figure 8. Linkage between the temperature increases and altitudinal glacier*
1087 *distribution. The 0 °C isotherms corresponding to the mean monthly minimum and*
1088 *maximum temperature are plotted for the 1994 and 2013 years according the observed*
1089 *T trends and lapse rates.*

1090

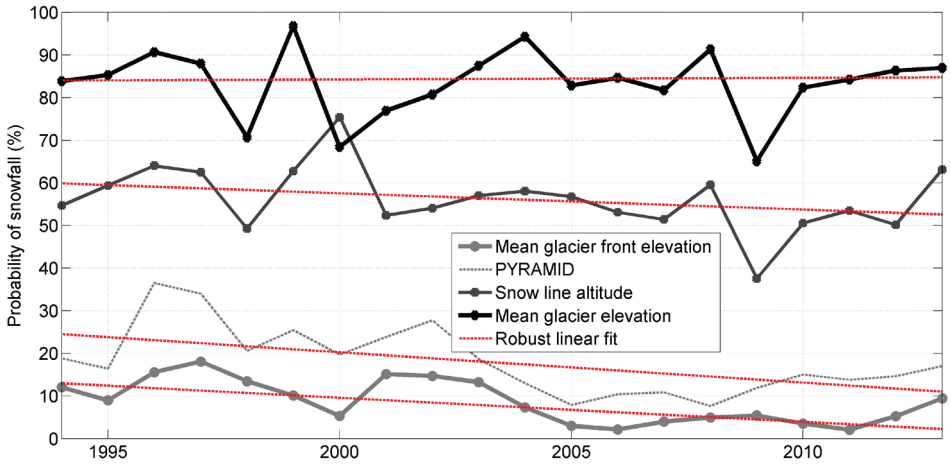

Figure 9. Trend analysis of annual probability of snowfall on total cumulated precipitation. The red lines represents the robust linear fitting of the time series characterized by the associated Sen's slope (more details in the caption of Fig. 3).